GEAP-4560
AEC RESEARCH AND
DEVELOPMENT REPORT
FEBRUARY, 1964

MECHANICAL, FLUID FLOW, AND HEAT TRANSFER OUT-OF-PILE TESTS ON EVESR MK1 PROTOTYPE FUEL BUNDLE

E.E. POLOMIK
J.R. FRITZ
P.W. IANNI

U.S. ATOMIC ENERGY COMMISSION
CONTRACT AT(04-3)-189
PROJECT AGREEMENT 29

ATOMIC POWER EQUIPMENT DEPARTMENT
GENERAL ELECTRIC
SAN JOSE, CALIFORNIA

GEAP-4560
AEC Research
and Development
Report
February 1, 1964

MECHANICAL, FLUID FLOW, AND HEAT TRANSFER OUT-OF-PILE TESTS ON EVESR MK I PROTOTYPE FUEL BUNDLE

E. E. Polomik
J. R. Fritz
P. W. Ianni

U. S. Atomic Energy Commission
Contract No. AT(04-3) - 189
Project Agreement 29

ATOMIC POWER EQUIPMENT DEPARTMENT
GENERAL ELECTRIC
SAN JOSE, CALIFORNIA

1742-TIO
3/64

TABLE OF CONTENTS

LIST OF ILLUSTRATIONS

LIST OF ILLUSTRATIONS (Continued)

LIST OF TABLES

SECTION I

SUMMARY

An EVESR MKI prototype fuel bundle was fully instrumented and operated intermittently for a 5-month period at the Pacific Gas and Electric Company's Moss Landing Power Station. The vessel was operated up to 1000 psi with steam flows from 2000 to 26,600 lb/h, and steam inlet temperatures up to 825°F. Data was recorded for blowout, vibration, flow distribution, heat transfer, and pressure drop.

The mechanical integrity of the fuel bundle, riser, and jumper system was satisfactory and considered to be of adequate design. No significant vibrations were noted during the various phases of operation.

Average flow distribution in three of the nine tubes showed an average variation of 5 percent from equal distribution. The center and corner tubes were low and the side tube was high. Maximum deviation, from an equal one, measured 12 percent.

Blowout of the flooded fuel bundle was accomplished with dry or significantly wet 1000 psia inlet steam, that steadied out to a minimum flow of 1250 lb/h. Blowout times were estimated at less than a minute for all flows above 1250 lb/h, and times in the vicinity of 2000 lb/h were estimated to be in the order of 5 to 15 seconds. Once the bundle was blown out a flow of 700 lb/h was sufficient to keep the fuel passages clear. This was true even with steam estimated at 10 to 20 percent wet.

Flows below 1250 lb/h caused partial blowout. Usually the A tube blew out first and the B and C tubes gradually cleared as flow was increased. Loss of flow then caused comparatively sudden flooding ranging from less than 2 to 3 seconds to several minutes for the different tubes within the bundle.

Once the bundle was blown out and the flow maintained at more than 700 lb/h, not enough water accumulated -- even with very wet steam -- to cause sudden flooding of all tubes when flow was cut off. Sudden flooding (i.e., in less than 2 to 3 seconds) occurred only in some tubes within the bundle, while others required times in the order of minutes to flood completely.

Heat transfer across the riser steam gap was found to be 12 to 30 times that calculated for a stagnant steam annulus. These results are consistent with estimates of increased heat transfer due to wire wrapping in the annulus and steam circulation. Radial wall temperature drops, at the top and bottom of the riser, varied from 10 to 30 F.

Pressure drop data and curves are presented for various segments of the fuel bundle and riser system. Total pressure drop was about 20 percent higher than estimated for saturated steam and was found to vary with the second power of the mass flow, indicating the strong effect of the expansion, contraction, and turn losses.

SECTION II

INTRODUCTION

To support the design of the EVESR nuclear superheater fuel bundle and jumpers it was decided to perform proof tests (out-of-pile) on a prototype Mark I fuel bundle. To proof test these components adequately, it was necessary to simulate test conditions as closely as possible to reactor operating conditions.

These tests were performed in a new test loop facility located at the Pacific Gas and Electric Company's Moss Landing Power Plant, where an adequate supply of high pressure superheated steam was available. This test loop was designed by the General Electric Co. and installed by PG&E's General Construction personnel.

The purpose of this report is: a.) to describe the design and operation of the test loop installed at Moss Landing Power Plant, b.) to describe the fuel bundle design and fabrication as well as the type of tests performed, and c.) to report the results of the fuel bundle tests.

A comparison of approximate EVESR fuel bundle operating conditions and anticipated test loop operating conditions are listed below.

	EVESR	Anticipated in Test Loop	Actual Maximum
1. Inlet Steam (Saturated)			
Pressure, psia	1000	1000	1000*
Temperature, °F	540	545 to 600	
Flow Rate, lb/h	3000 to 7000	30,000 Max.	23,000
2. Inlet Steam (Superheat)			
Pressure, psia	None	1000*	1000*
Temperature, °F	None	950*	900
Flow Rate, lb/h	None	2000 Max. *	7400
3. Outlet Steam			
Pressure, psia	950	900 to 980	
Temperature, °F	900 to 1000	540 to 600	900
4. Jumper Operating Temperature, F	900 to 1000	540 to 950	900

*Superheat steam flow through the prototype fuel bundle is in the opposite direction to that of the regular fuel bundle. This flow direction attempts to simulate temperature gradients in the jumper and riser.

		EVESR	Anticipated in Test Loop	Actual Maximum
5.	Process Tube Temperature, F	540 to 650	540 to 600	900
6.	Fuel Clad Temperature, F	540 to 1250	540 to 950	
7.	Jumper Length $\mathcal{L}$ Fuel to $\mathcal{L}$ of Outlet Pipe, inches	18-1/8 20-3/4 32-5/16	20	

SECTION III

DESIGN AND DESCRIPTION OF TEST EQUIPMENT

A. General Description of Fuel Bundle (See Figure 1, G.E. Drawing Number 104R651)

The EVESR Mark I (all-welded Type 304 stainless steel construction) prototype fuel bundle is an integral fuel unit consisting of a three-by-three fuel element (process tube, fuel rod, and velocity booster) configuration, a riser-downcomer section, and a coupling section with a total over-all length of 19 feet, 5 inches. This fuel bundle was fabricated at General Electric's Atomic Power Equipment Department, San Jose, California, to gain fabrication experience on the fabrication of the first core fuel for EVESR.

The fuel rods are supported by an upper tube sheet and are enclosed within stainless steel process tubes (welded to a lower tube sheet) that prevent the moderator water from mixing with cooling steam. Each of the fuel rods was filled with annular silver pellets rather than depleted UO_2 pellets or lead pellets. Approximately 165 lbs of silver were used in the prototype fuel bundle. The selection of silver was based on the following reasons:

1. UO_2 was not used in any form because of licensing and system contamination problems.

2. Silver has a density of 656 lb ft^3 compared to a UO_2 density (94 percent theoretical density) of 649 lb ft^3.

3. The coefficient of thermal expansion of silver ($10.9 \cdot 10^{-6}$) is slightly higher than stainless steel ($10.0 \cdot 10^{-6}$). This property would prevent fuel rod outer clad wrinkling type failures resulting from external pressure loading at elevated pressure.

4. The melting point of silver is 1761 F, as compared to the melting point of lead of approximately 500 to 650 F, which was adequate for operation of the test loop up to 950 F.

5. The net cost of silver metal was about $.06 oz which was based on an initial cost of $.92/oz minus a recovery cost of $.06 oz (when returned to the vendor for credit).

The plan used in instrumentation of the fuel bundle was to highly instrument the three typical types of fuel rods [identified as A, B, and C on Figure 1 (Drawing Number 104R651)]; i.e., the corner, side, and center tubes. The instrumentation used in the fuel bundle is shown on the drawings and sketches in the appropriate following sections.

B. Design and Construction of Test Loop

The out-of-pile test loop is physically located adjacent to the steam separation test loop; both loops are at the Moss Landing Steam Power Plant of the Pacific Gas and Electric Co. Figure 2 shows the entire piping and vessel arrangement. Superheated steam at 1350 psig and 950°F, and feedwater at 2000 psig and 380 F, are available from the power plant.

The main components of the test loop are shown on Figures 3 and 4 (G. E. Drawings Numbers 198E267 and 198E297), and consist of the following:

1. A Type 316 stainless steel vessel 12 inches in diameter by 24 feet long, designed for a working pressure of 1070 psig at 950 F. This vessel has a 6-inch pipe loop at its lower end to allow for natural circulation of water past the fuel bundle.

2. A Type 316 stainless steel thermal nozzle, which simulated the exit piping from the EVESR. The thermal nozzle, complete with strain gauges, was originally designed for a working pressure of 1000 psig at 950 F, but due to the substitution of a Type 316L rather than a Type 316 stainless steel 6-inch by 3-inch reducer during the fabrication cycle, it was necessary to reduce the rating to 1000 psig at 725 F. This rating reduction was accepted by Engineering because:

   a. To rework this thermal nozzle would have destroyed approximately 12 strain gauges and would have delayed the completion of the test loop startup by 1 to 2 months because of strain gauge and Type 316 stainless steel reducer procurement problems,

   b. The installation of a thermal liner inside the inlet to the thermal nozzle would make it possible to pass superheated steam up to 950 F without exceeding the rating of the nozzle, and

   c. Thermocouples could be attached to three points on the 6-inch by 3-inch reducer to monitor the temperature of this section.

      NOTE This section of the vessel can be coded at 1000 psig at 950 F by replacing the Type 316L stainless steel with a Type 316 stainless steel reducer.

3. A 2-1/4 percent chromium - 1 percent molybdenum piping system for the steam supply to the vessel.

4. A carbon steel piping system for the steam discharge lines to an atmospheric blow-down tank.

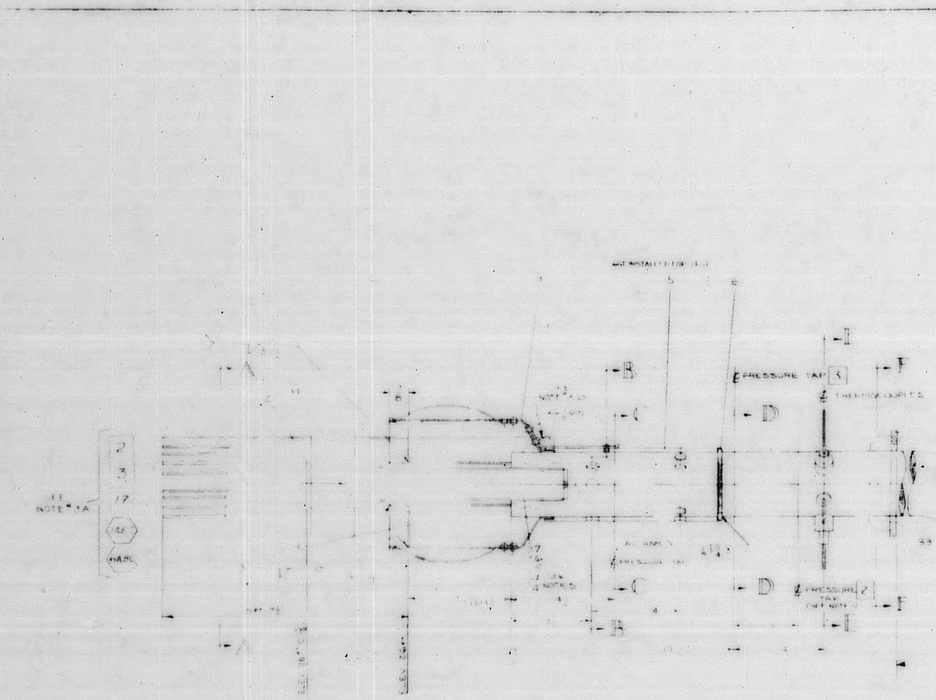
PRESSURE TAP
THERMOCOUPLES
SECTION B-B
SECTION A-A
SECTION F-F
SECTION J-J
SECTION H-H
1¼ SCH 5 PIPE
2½ OD-.065 WALL TUBING
2 OD-.065 WALL TUBING
SCRIBE LINE ½ MAX.
4 PLACES AT 90° ± ½° INTERVALS
TYP
SEE DWG 1986

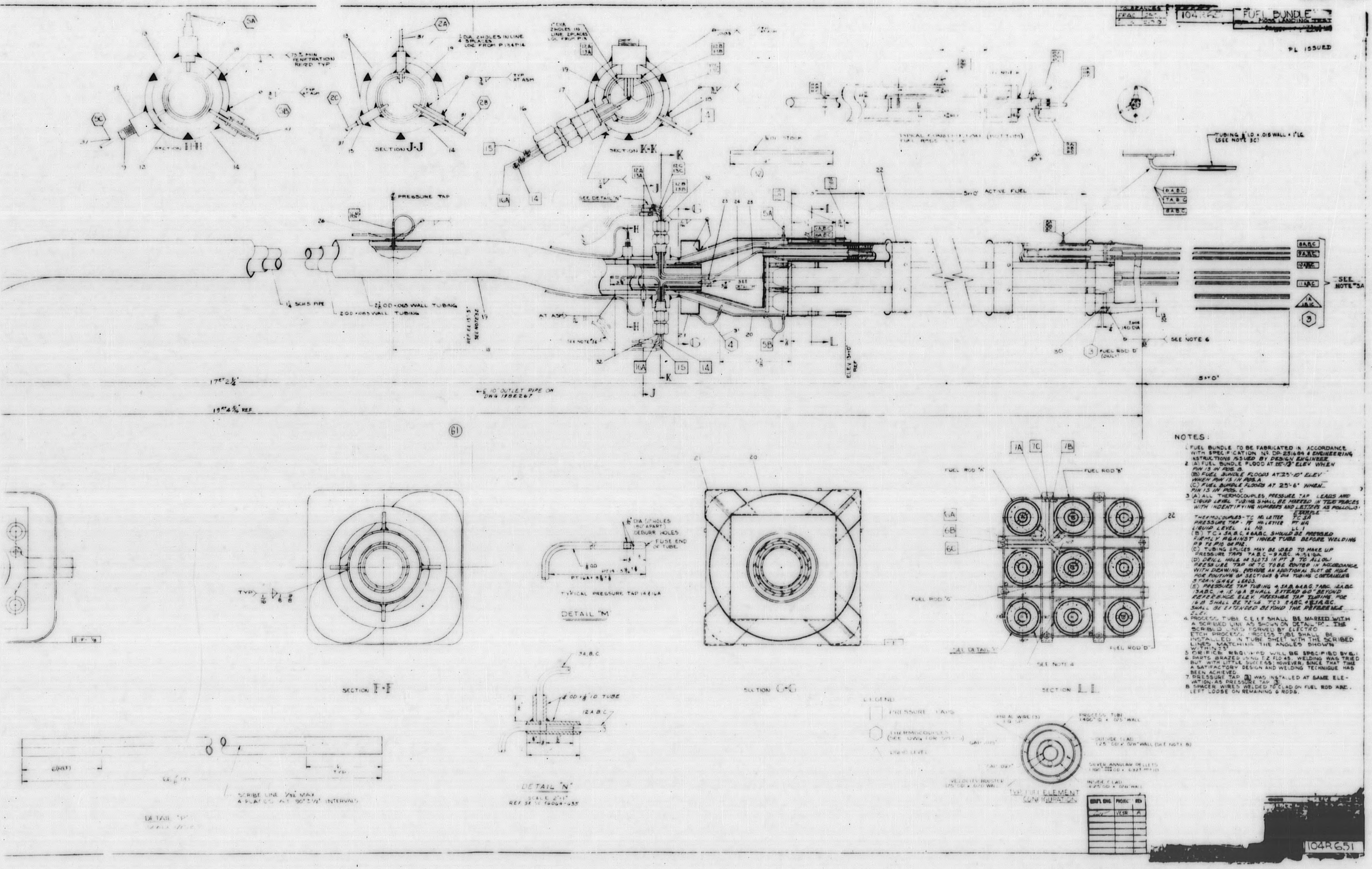

NOTES:

1. FUEL BUNDLE TO BE FABRICATED IN ACCORDANCE WITH SPECIFICATION NO. DP-251-004 & ENGINEERING INSTRUCTIONS ISSUED BY DESIGN ENGINEER.
2. (A) FUEL BUNDLE FLOOD AT 28'-7" ELEV. WHEN PIN IS IN POS. B.
   (B) FUEL BUNDLE FLOODS AT 25'-10" ELEV. WHEN PIN IS IN POS. A.
   (C) FUEL BUNDLE FLOODS AT 25'-6" WHEN PIN IS IN POS. C.
3. (A) ALL THERMOCOUPLES, PRESSURE TAP LEADS AND LIQUID LEVEL TUBING SHALL BE MARKED IN TEN PLACES WITH IDENTIFYING NUMBERS AND LETTERS AS FOLLOWS:

	EXAMPLE
THERMOCOUPLES - TC NO. LETTER	TC 3A
PRESSURE TAP - PT NO. LETTER	PT 8A
LIQUID LEVEL - LL NO.	LL 1

   (B) TC's 3A, B, C, & 8A, B, C, SHOULD BE PRESSED FIRMLY AGAINST INNER TUBE BEFORE WELDING PT TO PROCESS TUBE.
   (C) TUBING SPLICES MAY BE USED TO MAKE UP PRESSURE TAPS 7A, B, C - 9 A, B, C, & 16A.
   (D) DRILL HOLE OR SLOT IN PT 2 TO ALLOW PRESSURE TAP OR TC TO BE ROUTED IN ACCORDANCE WITH DRAWING. PROVIDE AN ADDITIONAL SLOT OR HOLE FOR ROUTING AT SECTION G & DIA TUBING CONTAINING STRAIN GAGE LEADS.
   (E) PRESSURE TAP TUBING 4, 5A, B, & C, 6A, B, C, 7A, B, C, 8A, B, C, & 16A SHALL EXTEND 60" BEYOND REFERENCE ELEV. PRESSURE TAP TUBING FOR 16B SHALL BE 72" & TC'S 3 A, B, C, & 8 A, B, C, SHALL BE EXTENDED BEYOND THE PRESSURE TAP LEVEL.
4. PROCESS TUBE C, E, & F SHALL BE MARKED WITH A SCRIBED LINE AS SHOWN ON DETAIL "D". THE SCRIBED LINE FORMED BY ELECTRO ETCH PROCESS. PROCESS TUBE SHALL BE INSTALLED IN TUBE SHEET WITH THE SCRIBED LINES MATCHING THE ANGLES SHOWN WITHIN 1°.
5. ORIFICES REQUIRED WILL BE SPECIFIED BY G.E.
6. PARTS BRAZED USING T.Z. FLO 45. WELDING WAS TRIED BUT WITH LITTLE SUCCESS; HOWEVER, SINCE THAT TIME A SATISFACTORY DESIGN AND WELDING TECHNIQUE HAS BEEN ACHIEVED.
7. PRESSURE TAP 8A WAS INSTALLED AT SAME ELEVATION AS PRESSURE TAP 3A.
8. SPACER WIRES WELDED TO CLAD ON FUEL ROD A, B, C, LEFT LOOSE ON REMAINING 6 RODS.

Figure 1. EVESR MKI Prototype Fuel Bundle (G. E. Drawing 104R651)

GENERAL ELECTRIC 762D780

TITLE PROTOTYPE TEST
ISOMETRIC PIPING ARRANGEMENT
FIRST MADE FOR MOSS LANDING

762D780

LEGEND

- (P) PRESSURE GAGES
- (T) TEMPERATURE SENSING DEVICES
- NORMAL STEAM FLOW

NOTE 1. SUBSTITUTION OF 316 L STN STL INSTEAD OF SPECIFIED 346 STN STL REDUCED DURING MFG. CYCLE DETERMINED RATING OF THERMAL NOZZLE.

Figure 2. Piping and Vessel Assembly Isometric (G. E. Drawing 762D780)

APED SAN JOSE 762D780

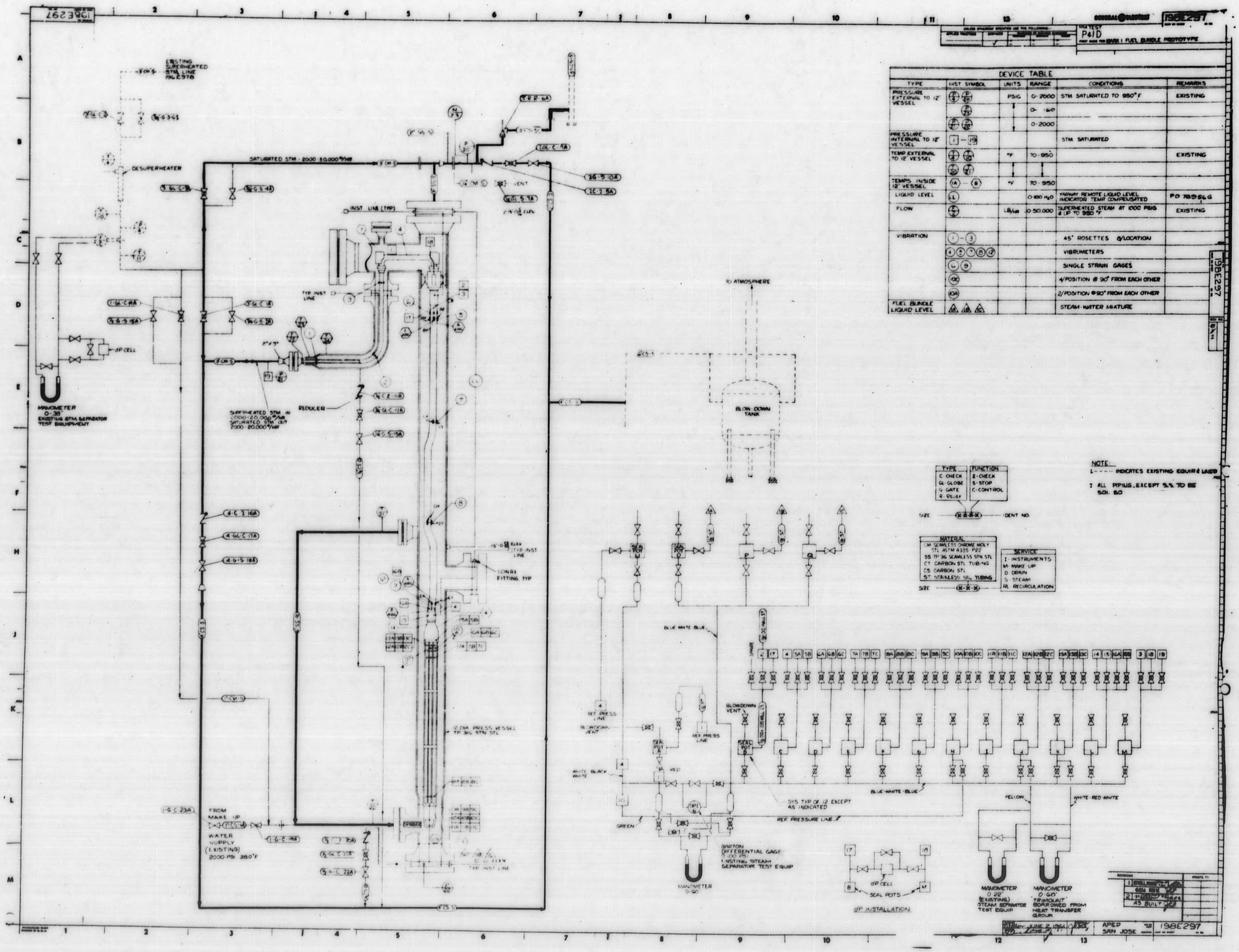

Figure 3. Test Loop (G. E. Drawing 198E297)

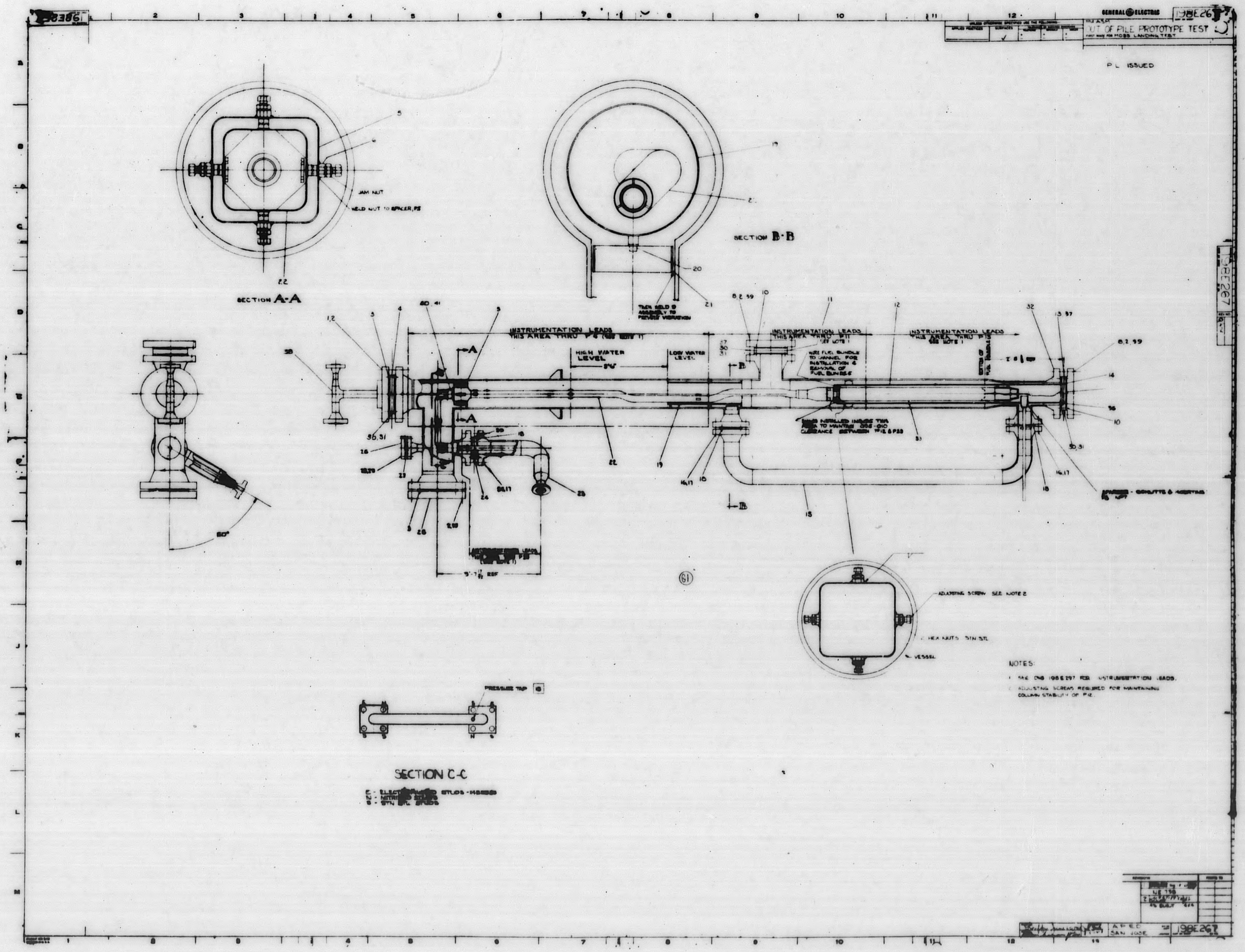

Figure 4. Vessel and Fuel Bundle Assembly
(G. E. Drawing 198E267)

5. A stainless steel EVESR prototype fuel channel which supports the prototype fuel bundle.

6. A stainless steel channel which supports and positions the prototype fuel channel.

7. A prototype jumper.

8. A structure for supporting the test loop equipment. This structure has three grating levels above ground level which are connected by an outside safety-cage-type ladder. Located on the different levels are seal pots and other types instrumentation.

9. Instrumentation consisting of seal pots, thermocouples, portable potentiometers, and Brown recorder, manometers, pressure gauges, instrument tubing and valves. Two 60-inch manometers, were borrowed from the test group located in Building G.

C. Thermocouple and Pressure Tap Data

Thermocouples were 1/8 inch OD sheathed in Type 304 stainless with Chromel-Alumel wires. Location of the thermocouples is shown on Figures 1 and 5.

THERMOCOUPLE NUMBERING SCHEDULE

Number on Figures 1 and 4	Brown Recorder Printing Number	Identification Number	Location and Purpose
1 A, B, C	1, 2, 3	1, 2, 3	Steam at top of fuel bundle riser
2 A, B, C	4, 5, 6	4, 5, 6	Steam at bottom of riser
3	16	16	Steam or water at bottom of fuel bundle
4	8	7	Steam in outer plenum between riser annulus and fuel downpass
5 A, B, C	9, 10, 11	8, 9, 10	Lower outer riser wall temperature
6 A, B, C	12, 13, 14	11, 12, 13	Upper outer riser wall temperature
7	15	17	Steam at inlet to riser annulus downpass
21			Outer wall temperature at side-leg flange
22			
23	7		Outer wall temperature at thermal nozzle outlet
24			
25		15	Steam or water at bottom of vessel

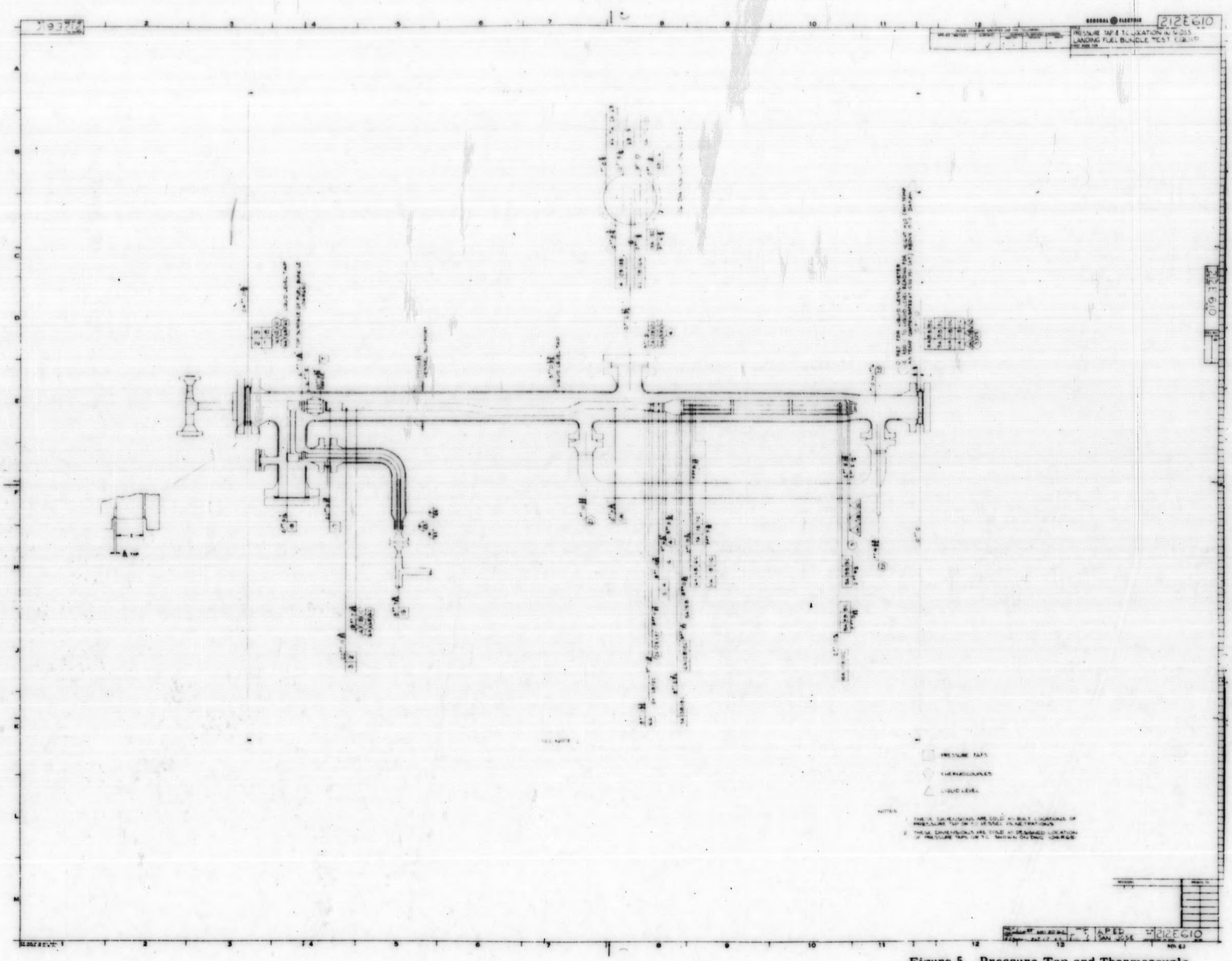

Figure 5. Pressure Tap and Thermocouple Locations

SECTION IV

GENERAL OBJECTIVES AND DESCRIPTION OF TESTS

The principal objectives of the test program are summarized below. Additional description and discussion may be found in the relevant subsections of Section VI, Results.

a. Mechanical Integrity

General adequacy of the MK I fuel bundle from a pressure, thermal cycling, and temperature standpoint with a destructive examination of components following the tests.

Evaluation of design of jumper materials and ease of assembly and disassembly after high-temperature operation.

b. Blowout

Flows and times for clearing and maintaining bundle free of water.

c. Flow Distribution among the nine tubes comprising the bundle.

d. Heat Transfer rates between hot steam in the riser tube and the cooler steam in the inlet annulus.

e. Pressure Drop of the entire system.

SECTION V

FLOW DATA REDUCTION

Orifice plates, 0.710 and 2.450 inches thick, were used in the vertically-oriented flange. Mercury, and Merriam Blue and Red oils (nominal specific gravity of 1.75 and 2.95, respectively) were used in a high-pressure 60-inch manometer for the flow ranges covered.

The basic equation recommended by the ASME Fluid Meters[1] was used to calculate mass flow, in the vertical orifice F2 installation shown on Figures 1 and 2, for all of the runs. The equation used for runs through May 23, 1962, was

$$W = 45.47\, Y K D_o^2 \left[1 + \frac{20}{10^6}(T_s - 75)\right] \frac{1}{v} \sqrt{M\rho_1\left[\frac{\rho_2}{\rho_2} - 1\right] - 2.38\,(\rho_f - \rho)} \quad (1)$$

Nomenclature is as follows:

W = lb/h, mass flow

Y = Expansion factor, reference 1;

K = Orifice coefficient, reference 1;

D_o = Inches, ID of orifice at 75 F;

T_s = F, steam temperature at orifice;

v = ft^3/lb, steam at orifice Temperature T_s, and Pressure P_4;

M = Inches, manometer reading;

ρ_1 = lb/ft^3, water density at room temperature and P_4;

ρ_2 = gms/cc, density of manometer fluid, and water respectively, at room temperature and pressure; and

NOTE The specific gravity of the manometer fluid was read from reference 2 at room temperature and pressure and the assumption was made that compressibilities of fluid and water were about the same.

ρ_f = lb/ft^3, saturated water at P_4 or P_{20}

The 2.38-inch dimension in Equation (1) is a vertical water leg correction maintained until May 23, 1962. The orifice legs were readjusted on that date and a new dimension, 2.50 inches, was maintained thereafter.

Thus, after May 23, 1962, Equation (2) below was used for calculation of flow

$$W = 45.47\, Y K D_o^2 \left[1 + \frac{20}{10^6}(T_s - 75)\right] \frac{1}{v} \sqrt{M\rho_1 \left[\frac{\rho_1}{\rho_2} - 1\right] - 2.50\,(\rho_f - v)} \qquad (2)$$

Figures 6 and 7 were made up for quick estimation of the flow, with the various orifices and manometer fluids, during operation. The charts are quite accurate if used carefully. W(P*) on Figure 6 is the saturated flow for the orifices and manometer readings shown, with Y assumed as 1 which was within 1 2 percent for the runs made. The 1,000-psi curve on Figure 7 is then entered at the $v_{P,T}$, for the actual temperature at the orifice, to obtain a correction factor, F. Then actual flow at conditions

$$W_{P,T} = \left[F\left(\frac{P^*}{v_{P,T}}\right)\right]\left[W(P^*)\right]. \qquad (3)$$

Curves, similar to Figure 6, but for other operating pressures, were available. These, together with Figure 7, with interpolation at odd pressures as necessary, provided adequate setting or estimates of the flow rates.

Properties of steam, except thermal conductivity, and water were taken from reference 3. Thermal conductivity of steam was taken from the data of reference 4.

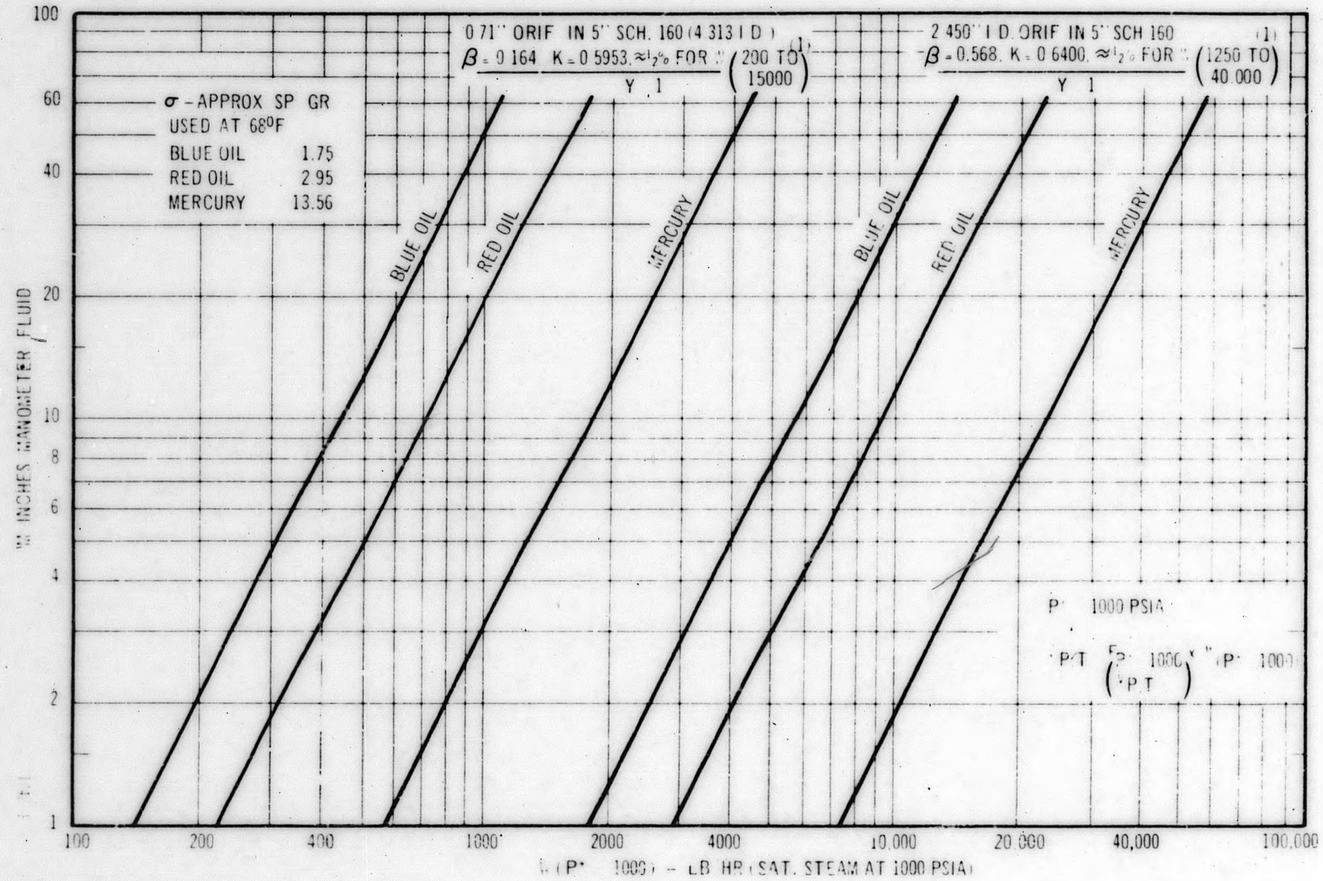

Figure 6. Saturated Steam Mass Flow

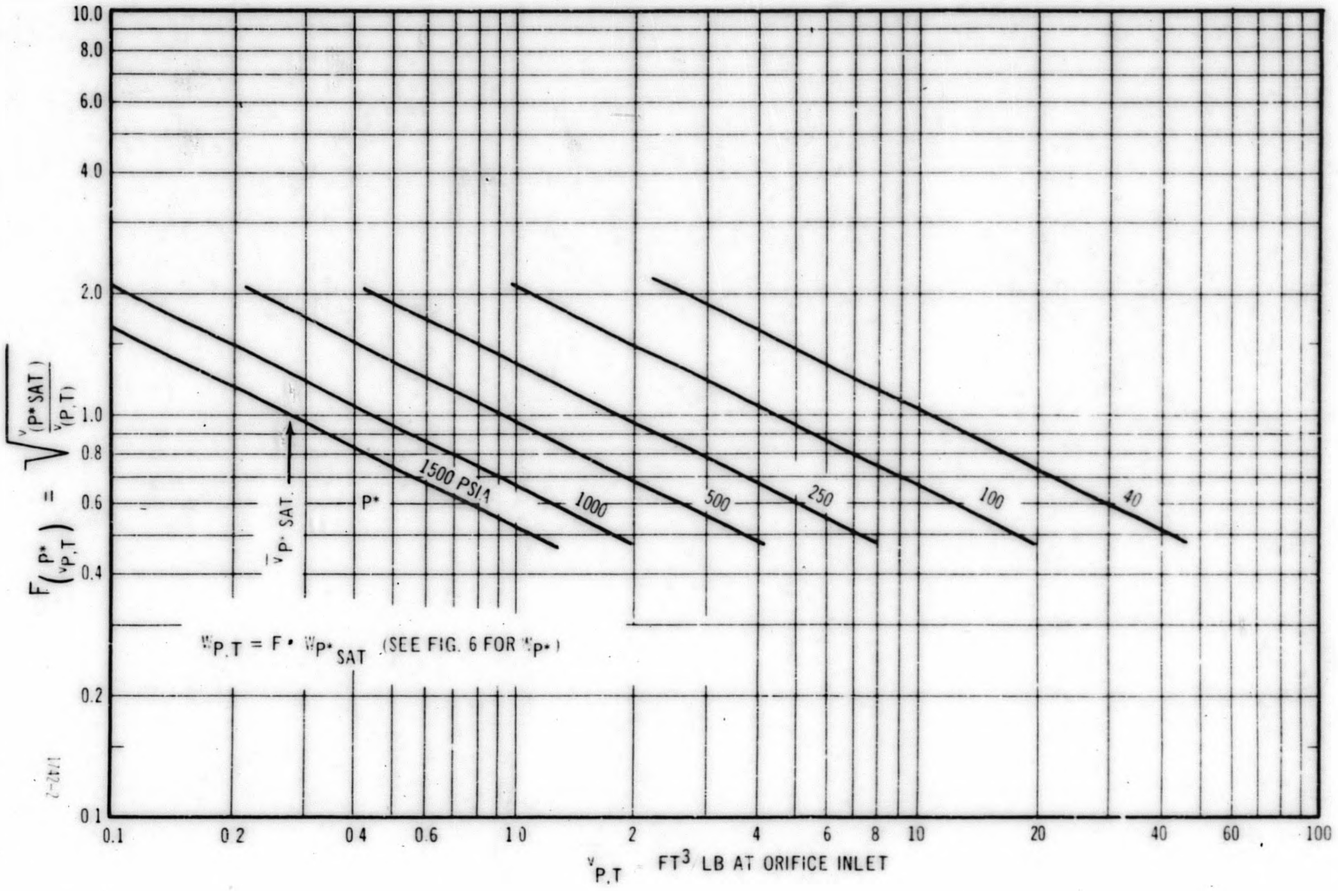

Figure 7. Steam Flow Correction Factor

SECTION VI

RESULTS AND DISCUSSIONS

A. Summary of Runs

Table I is a summary of all the runs showing date, flow, pressure, and steam inlet temperature, and type of data taken during each run.

Due to the large amount of data available, it was not necessary to reduce all of it to obtain adequate results. Thus, indication of certain type data under a run does not mean that results for that particular run will be found reduced in following sections.

B. Mechanical Integrity of Test Loop

The test loop was operated intermittently during a 5-month period from April to September, 1962. Tests were scheduled in cooperation with the Mechanical Development unit of Development Engineering (which also performed tests during this period) and the PG&E operating group. Operation of the test loop is explained in Appendix A.

A summary of vessel operation was as follows:

1. The vessel was heated from room temperature to pressure and temperature a total of 31 times.

2. Steam Flow Through Fuel Bundle

	lb/h	Hours
Flow in normal direction	2000	33
Flow in normal direction	2000 to 3000	20
Flow in normal direction	3000 to 4000	25
Flow in normal direction	4000 to 5000	21
Flow in normal direction	5000 to 6000	5-1/2
Flow in normal direction	7000 to 8000	9-1/2
Flow in normal direction	10,000 to 11,000	9
Flow in normal direction	12,000	1/2
Flow in normal direction	15,000	2-3/4
Flow in normal direction	20,000	1/2
Flow in normal direction	25,000	2/3
Flow in normal direction	26,600	2/3
Flow in reverse direction	2000 (650 to 825°F)	7-2/3

TABLE I

SUMMARY OF RUNS, FLOWS, AND TYPE DATA TAKEN

Date (1962)	Run Number	P_{20} Heise (psia)	Orifice Steam Temperature $T_s - T_{10}$ (°F)	W lb h · 10^{-3}	Type Data Taken: Blowout	Pressure Drop	Flow Distribution	Heat Transfer	Condensation Flooding
4 24	101	1040	578	5.62		√			
4 25	103	975	560	10.72		√			
4 26	106	127	338	2.72		√			
4 27	108	1003	570	8.47		√			
4 27	109	926	589	13.37		√			
4 27	110 cf to 106	125	357-367			√			
5 7	204	975	604	3.45	√				
5 7	205	995	est. by T7 560	3.61	√				
5 7	206	990	540 Sat.	3.75	√				
5 9	308	982	549	3.66	√				
5 10	209 A B C	971	547	0.64	√				
5 10	210	985	587	1.53		√			
5 10	211 B	1003	555	1.18	√				
5 11	212 B	1008	575	1.27	√				
5 11	213 A	995	580	3.98					
5 21	214 A B C	518	505	2.69	√				

TABLE I (Continued)

Date (1962)	Run Number	P_{20} Heise (psia)	Orifice Steam Temperature $T_s - T_{10}$ (F)	W lb h · 10^{-3}	Type Data Taken: Blowout	Pressure Drop	Flow Distribution	Heat Transfer	Condensation Flooding
5 21	215A	520	505	3.90					
	B		est. by T7-214						
5 21	216A	520	475	0.42					
	B								
5 21	217A	520	515	2.03					
	B								
5 22	218A	1020	568	1.31					
	B	1008	580	1.30					
	C	1015	560	1.31					
5 22	219A	1000	550	2.79					
	B	1005	580	2.79					
	C	1013	585	2.68					
5 24	220	1012	583	9.88					
5 24	221	1012	580	5.49					
5 25	222A	1010	550	0.47					
	B	1000	540	0.46					
	C	1000	540	0.44					
	D	1000	545	0.43					
	E	1005	550	0.46					
5 25	225A	1010	605	1.62					
	B	1010	545	1.64					
			fairly wet						
	C	1010	545						
			sat. x ?	0.75					
6 4	226	970	590	1.08					
		970	590	1.40					
6 4	227	995	550	2.13					
6 5	228	981	548	0.81					
6 5	229	985	596	0.50					

TABLE I (Continued)

Date (1962)	Run Number	P_{20} Heise (psia)	Orifice Steam Temperature $T_s - T_{10}$ (F)	W lb h · 10^{-3}	Type Data Taken				
					Blowout	Pressure Drop	Flow Distribution	Heat Transfer	Condensation Flooding
6 5	229	985	596	1. 21					
6 5	229	985	596	0. 77					
6 8	230	970	540 wet	0. 70					
6 8	231	970	543 wet	0. 78					
6 8	232								
6 8	233	970	570	1. 52					
6 8	233	970	540 wet	1. 27					
8 27	234	1015	649	5. 20					
8 28	235	1013	662	6. 11					
8 28	236	1014	660	4. 21					
8 29	237	1017	645	3. 34					
8 29	238	1013	669	2. 48					
8 29	239	1011	654	5. 21					
8 30	240 A-Q								
9 10	245	1021	672	2. 04					
9 10	246	1014	653	3. 11					
9 11	249	1005	793	2. 10					
9 11	250	1014	790	2. 14					
9 11	251	1014	775	2. 14					

TABLE I (Continued)

Date (1962)	Run Number	P_{20} Heise (psia)	Orifice Steam Temperature $T_s = T_{10}$ (°F)	W lb h · 10^{-3}	Type Data Taken				
					Blowout	Pressure Drop	Flow Distribution	Heat Transfer	Condensation Flooding
9/11	252	1015	770	2.94					
9/11	253	1015	765	2.98					
9/12	254	1015	775						
	255	1016	775	4.79					
9/12	256	1015	775	4.85					
9 12	257	1016	775	4.84					
9 12	258								
9 12	259	1016	794	5.61					
9/12	260	1015	800	6.75					
9 12	261								
9 12	262	1015	790	6.76					
9 12	263	1012	658	7.39					
9/12	264	1012	663	6.13					
9 12	265	1011	655	5.19					
9 13	266	1014	665	4.25					
9 13	267	1011	654	5.10					
9 13	268	1014	653	6.19					
HIGH FLOWS FOR MECHANICAL INTEGRITY									
9 14	269	1006	650 est.	13.37					
	270	1012	655 est.	13.37					

TABLE I (Continued)

HIGH FLOWS FOR MECHANICAL INTEGRITY (Continued)									
					Type Data Taken				
Date (1962)	Run Number	P_{20} Heise (psia)	Orifice Steam Temperature $T_s - T_{10}$ (°F)	W lb h · 10^3	Blowout	Pressure Drop	Flow Distribution	Heat Transfer	Condensation Flooding
9 14	271	$\overline{1011}$	660 est.	18.41					
9 14	272	$\overline{1015}$	645 est.	23.03					
9 14	273	$\overline{1017}$	628 est.	23.91					

	lb/h	Hours
Flow in reverse direction	3000 (650 to 825 F)	1-1/4
Flow in reverse direction	4000 (650 to 825 F)	7-1/2
Flow in reverse direction	5000 lb/h (650 to 825 F)	2-1/2
Flow in reverse direction	6000 lb/h (650 to 825 F)	2-3/4
Total hours steam flow through Fuel Bundle		149

3. During operation there were a number of problems which occurred which can be corrected by an improvement in design. These are enumerated below.

   a. The feedwater supply line which supplies makeup water to the vessel should be lagged and a bypass line should be installed which will permit draining this line prior to usage. At present about 100 to 150 feet of this line are unlagged, which permits the feedwater temperature to range from 50 to 380 F.

   b. The connection between the feedwater supply header (carbon steel pipe) and the stainless steel line to the vessel should be changed from the present union to a flange-type joint. The union has started to leak and probably will continue to do so. It probably should not have been used for this service.

   c. The tubing to the seal pots should be 300 series stainless steel rather than the carbon steel currently in use. The carbon steel corrodes quite rapidly in the atmosphere at Moss Landing.

   d. The 3-inch steam supply line from the building to the F-2 orifice should be covered with more insulation if a temperature higher than 825 F is desired. Temperature of the steam from the boiler may vary from 875 to 950 F (1350 psig) and will depend on the operation of the steam plant.

   e. The structure supporting the vessel should be painted.

   f. The 6-inch thermal nozzle should be removed and the 6-1/3-inch reducer replaced to increase the over-all pressure-temperature rating of the vessel.

4. Bolts used to fasten the blind flanges of the vessel together were wrapped with Teflon tape to minimize galling of the threaded joints. Threaded Conax fittings wrapped on the threaded end with Teflon tape did not develop a single leak during operation of the loop.

5. There were a number of instrument equipment failures during the operation of the test loop; these are listed below:

   a. Three metal sheathed (Type 304A stainless steel) thermocouples (6A, B, C) started to weep water on September 14, 1962, which indicated a sheath break had occurred. The point at which this breakage occurred was not determined.

   b. Strain gauges, which were spot welded to the fuel bundle and to the thermal nozzle outlet line, started to leak steam after a few hours operation at temperature and pressure. All strain gauge leads leaked steam before test loop was shut down. Leaks were plugged by pinching ends shut and then silver soldering.

   c. Pressure tap number 18 broke off and was lost in system during the early test runs. This pressure tap, which was attached to the jumper, was replaced, but during the first test erroneous readings were being obtained. Upon removal of the jumper at the conclusion of the tests it was noted that the 1 8-inch OD by 0.015-inch wall stainless steel tube had split. The stainless steel tubing appeared to be quite brittle.

   d. Pressure tap number 11A inside the vessel had a small pin-hole leak in the tubing when the fuel bundle was being removed from the vessel.

   e. Vibrometer assemblies leaked steam during the first days of operation. It was believed this leakage occurred at a screwed pipe joint.

6. Destructive examination of the fuel bundle was performed in the following manner:

   a. The riser downcomer section was cutoff about 14 inches above the outside reducer section.

   b. The 14-inch section of the riser downcomer was removed from the reducer section. This section contained the Pitot-static tubes.

   c. The outside reducer section was cutoff.

   d. The inside reducer section was cutoff and the thermal sleeve removed.

   e. The lower tube sheet and support frame were removed.

   f. The upper tube sheet was sawed so that individual fuel rods could be separated from each other.

g. The nose-piece removed.

h. The process tube end plugs were cutoff and removed. The velocity boosters and fuel rods A, B, and C were removed with process tube end plug.

i. The individual fuel rods were removed from the process tubes.

j. The fuel rod outside cladding was cut longitudinally on a milling machine. The fuel rod lower end plug was cutoff and the upper end plug was separated from the outer clad. The upper end plug and inside clad were removed from the silver annular pellet column. The silver annular pellets were removed and returned to fuel manufacturing operation.

k. The lower tube sheet was sawed so that individual process tubes, as well as process tubes in two banks of three each, were removed.

7. Results of the destructive examination of the fuel bundle are listed below:

a. Fuel rod orientation is shown in Figure 8:

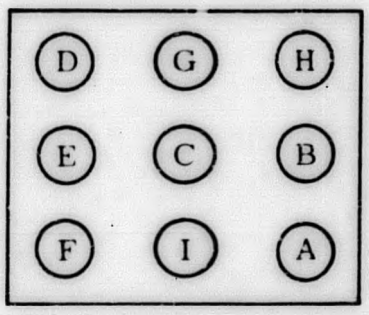

Figure 8. Fuel Rod Letter Designation and Orientation

Two of the three fins were lost from Pitot-static tubes A and B.

One of the three fins was lost from Pitot-static tube C.

One of the fins was located between the velocity booster and the inside clad near the bottom of the corner fuel rod adjacent to B. The remaining fins were never located and it was assumed they were blown out into the blow down tank.

b. The Uni-Clamp used to hold the instrumentation against the riser-downcomer assembly appeared to work satisfactorily.

c. The metal clamps spot welded to the process tube or downcomer and used to fasten the instrumentation in place appeared to work satisfactorily.

d. The use of E-Z flow 45 silver solder braze for fastening instrumentation to the fuel bundle appeared to work satisfactorily. Some of these joints did not take much physical abuse before they failed at the brazed section.

e. The process tube spacers which consisted of two layers of wire grids welded to an outer stainless steel sheet metal band appeared to perform the design function. Contact marks were noted on the outer band where the process tube was in contact with the spacer. Four 1/8-inch-diameter rods fastened the spacers together.

f. The inside reducer (5-3/16 inches square by 1/8 inch thick) was dished inward a maximum of 1/8 inch. The tapered section of this reducer was dished inward a maximum of 3/16 inch. This collapsing of the reducer was the result of an external pressure of about 630 psig which occurred during run number 273 which simulated an outlet-pipe-break-type accident. The thickness of this section was purposely left at 1/8 inch thick to see what would occur during the pipe-break-type accident.

g. Process tube end caps were cut off and inspected for potential metal particles, etc., which may have dropped into the system during manufacture. Nothing was noted in any of the process tube end caps.

8. Process Tube Examination.

a. Process Tubes A, F, and H looked very good on the outside surface. Rusty spots were noted on the tube where it was touching the sheet-metal band on the first spacer below the fuel bundle support frame.

b. Process Tube B had a depression 1/2 inch in diameter by 1/32 inch deep located 10 inches from the lower end of the tube. This depression was the result of damage incurred during manufacture of the fuel bundle. An attempt was made to remove the depression but with no success. A burned area about 1/4 inch in diameter by 5 to 10 mils deep (20 inches from lower end) resulted from improper grounding of electrodes during welding operations.

c. Process tubes C and G looked good on the exterior.

d. Process tubes D and E both had burned areas, 1/4 inch in diameter by 1 to 10 mils deep, on the exterior surface (19 to 20 inches from lower end of process tube) which resulted from improper grounding of electrodes during welding operations. The remainder of the tube looked good.

e. Process tube I was split into two halves to allow an examination of the process tube inside surface. Spiral wire contact points were noted along the length of the tube. The width of this contact ranged from 1 32 to 5 32 inch. No appreciable wear, if any, was noted. The spiral wires on the fuel rod were welded only to the lower and upper end plugs.

9. The velocity booster tubes, used in fuel rods A, B, & C, were the only ones examined. The tubes looked very good. No broken fusion welds were noted. The brazing of pressure tap tubes on velocity booster appeared to survive the test.

10. Fuel Rod Examination

a. Fuel rods A, B, and C, with full pressure tap instrumentation, were removed from the process tube without breakage of any wires. The wires were spot welded to the outside clad. Upon cutting these fuel rods open to remove the silver, it was noted that water had leaked into the fuel rod which was the result of burn-through of the clad when spot welding the wire to it. It is apparent that a satisfactory process for spot welding the wires to the clad has not been developed.

b. Fuel rods D through I, paragraph 8. a. above, had spiral wires welded to the bottom and upper end plugs. When the fuel rods were removed from their respective process tubes, it was noted that the following wires broke at the weld affected zones.

(1) One wire broken at upper end plug on fuel rods H, F, and I.

(2) Two wires broken at lower end plug on fuel rod E.

(3) Two wires broken at upper end plug on fuel rod G.

(4) Three wires broken at upper end plug on fuel rod D.

c. Spiral wire contact points on fuel rods D through I were noted along the length of the tube. The width of these contacts ranged from 1 16 to 1 8 inch. No appreciable wear, if any, was noted.

d. Upon removing silver from the fuel rods, it was noted that the silver pellets were free to slide in fuel rods D through I when they were turned upside down. It was noted that a maximum longitudinal gap between pellets of 5 32 inch could have existed in some fuel rods.

e. It appeared as though most of the wires which were welded to either the top or bottom end plugs were cracked near the weld affected zone.

11. Jumper Evaluation

The jumper used at Moss Landing was supposed to be the prototype for the EVESR reactor, but late in the design phase of the project it was decided to incorporate "Marman"-type conoseal joints rather than the metal-enclosed asbestos type gasket. The jumper was removed on four different occasions. All bolts were tightened to a torque of 30 ft-lb at installation, and were installed with no lubrication on the threads. On each occasion the bolts were checked to see if they had loosened during operation. For results see Table II. The jumper bolt details are shown in Figure 9.

From the limited tests performed at Moss Landing, all threaded assemblies appeared to operate satisfactorily with no galling on the threads which would permit seizing of the two mating surfaces.

Bolt Number and Material

1 - Electrolized/G. E. Specification FA 231911

2 - Nitrided/G. E. Specification FA 231909

3 - Type 304 Stainless Steel

4 - Type 304 Stainless Steel

5 - Type 304 Stainless Steel

6 - Electrolized G. E. Specification FA 231911

7 - Nitrided G. E. Specification FA 231909

8 - Type 304 Stainless Steel

TABLE II

TORQUE REQUIRED TO LOOSEN JUMPER BOLTS

Removed Jumper (Date)	TORQUE - FT-LBS Bolt No. 1	2	3	4	5	6	7	8	Remarks
April 28, 1962	10	F. T.	10	F. T.	F. T.	10	F. T.	10	See Note 1
May 16, 1962	F. T. *	F. T.	F. T.	10	F. T.	F. T.	10	F. T.	See Note 2
June 9, 1962	F. T.	F. T.	F. T.	F. T.	F. T.	F. T.	F. T.	F. T.	See Note 3
September 15, 1962	25	20	13	15	20	F. T.	27	23	See Note 4

*F. T. - Finger Tight

Notes:

1. Loosened bolts numbered 1, 3, 6, and 8; all others appeared to be finger tight. Bolts numbered 2, 6, and 8 had a tendency to gall.

2. Loosened bolts numbered 3 and 7; all others appeared to be finger tight. Nitrided thread on bolt number 7 appears to be scratched. Stainless steel threads on bolts numbered 3, 4, 5, and 8 appear to be galling.

3. All bolts appear to be loose.

4. Installed four carbon steel "Belleville" washers under head of bolts numbered 1, 4, 5, and 8 in patterns shown in sketch. Bolts were loosened in following sequence 1-4-2-3-5-8-7-6.

12. Vibration

No serious vibrations, or their effects, were noted during the normal operation of the loop up to 1000 lb/h.

C. Blowout

The purpose of the blowout tests was to determine the suddenly-admitted flows, and times, necessary to clear the tubes of water, and also the minimum flows necessary to maintain the tubes free of water after blowout.

1. Description

A manometer was connected with its reservoir at the bottom of the tubes and the top connected to taps (1) A, B, or C at the bottom of the process tubes. As water was blown out of the tube, the manometer reading decreased. The manometer readings then served as indicators for the level of liquid in the three unique tubes of the bundle.

A given flow was set in the system with flow bypassing the bundle to the blowdown tank. The inlet valve to the bundle and valve to blow down were then opened and closed simultaneously to admit flow through the bundle. Time of valving and manometer readings were recorded during the course of blowout to give a history of the liquid level in the tubes.

After blowout, the flows were shut off and manometer-time readings again recorded to determine rates of water filling or reflooding. Because of the vessel heat losses, condensation of the steam in the dome was a source of moisture causing reflooding, in addition to that still remaining somewhere within the bundle.

2. Results and Discussion

Shown in the following graphs are the principal results plotted as manometer-time curves; the degree of water level in the tubes is indicated. Minimum flow to blow out the fuel bundle was established at 1250 lb h with saturated steam flowing into the fuel bundle. Shown in Figure 10 (run number 229) are the manometer readings as a function of time as the flow rate was increased. Figure 11 is a plot of the same data, and that of run number 226, in which only one tube was monitored. At low flow, only one tube cleared, and as the flow was increased, the other tubes were also cleared. (This assumes all tubes behaved as the three instrumented tubes because of symmetry.) The data does not indicate what occurs transiently except that a surge lasting up to about 30 seconds was observed as water was forced out.

It is apparent that one tube clears first, and that the others remain partially flooded until sufficient flow is established to give enough pressure drop across the parallel tubes to blow them out also. This flow rate is less than that which gives a pressure drop equal to the static head of the parallel elements when all are cleared. This is probably because the blowing out process is inherently a transient phenomenon and it occurs as a step while some tubes are still partially flooded. Thus, at the instant when all the tubes cleared the actual ΔP, existing momentarily across the parallel elements, may have indeed exceeded the static head for a brief moment. The response time of the manometer

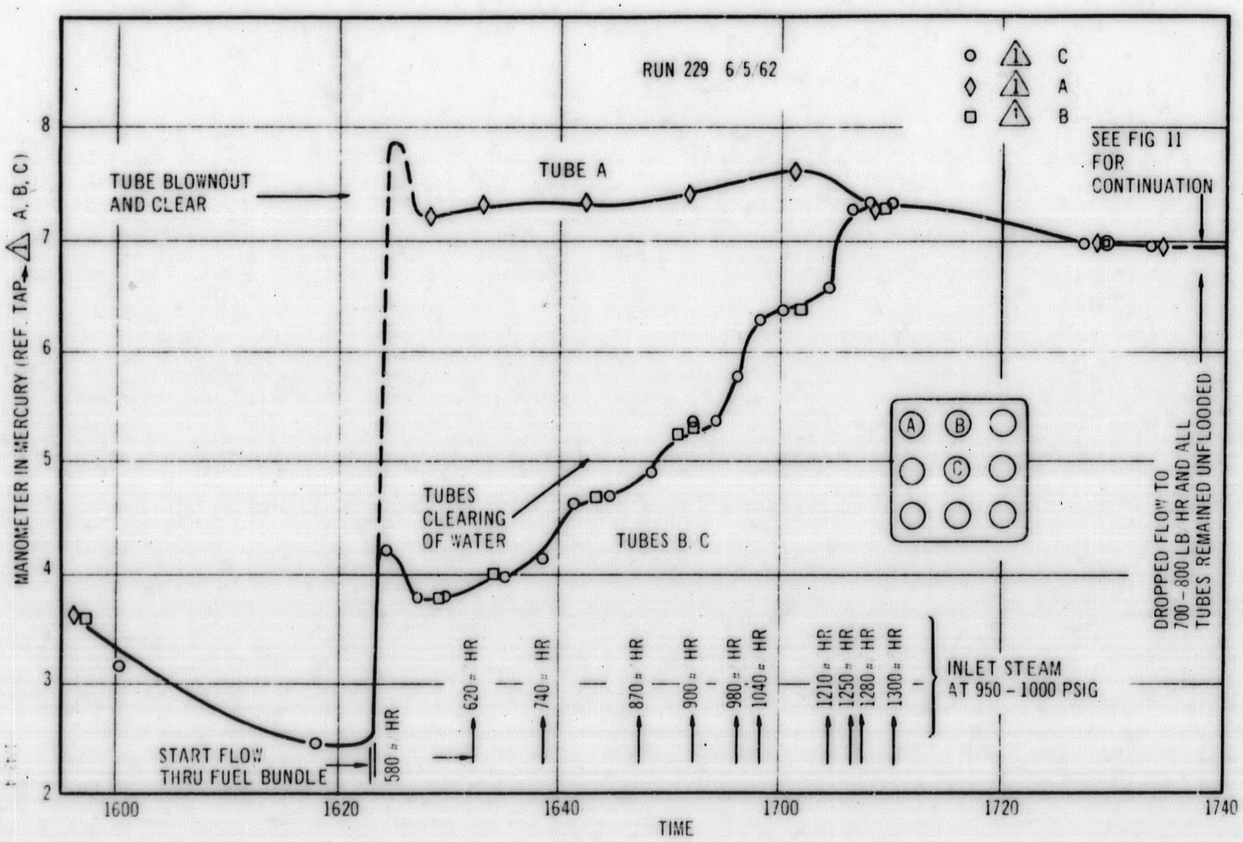

Figure 10. Blowout History vs Time and Flow

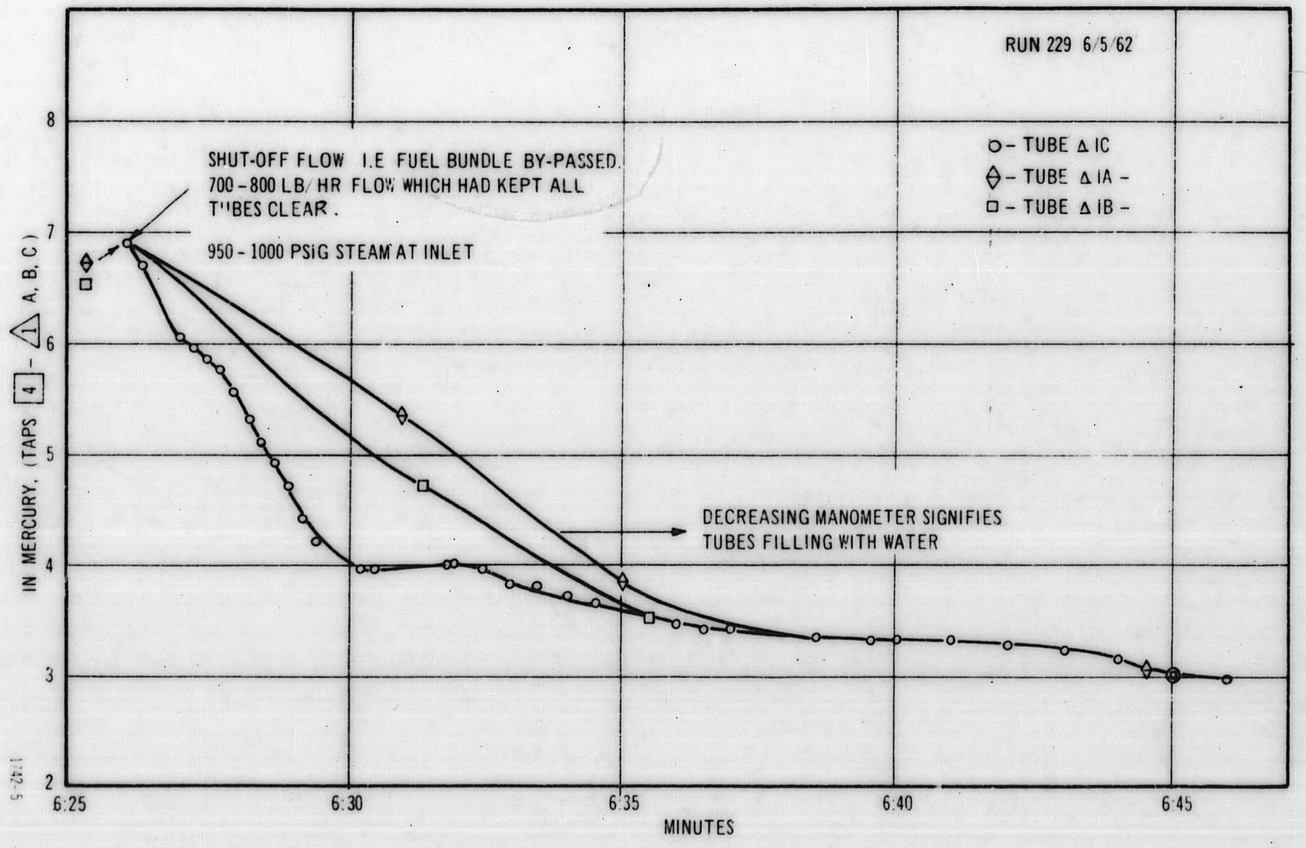

Figure 11. (Continuation of Figure 10), Filling Rate After Blowing Out with Minimum Blowout Flow (1250 lb/h)

system was too slow to study such transients. Pressure surges during the blowout process were under 150 psig for all the flows tested.

Shown in Figure 12 are the blowout conditions during runs numbers 226 and 229 (Figure 10) plotted against steam flow. It is noted that process tube A clears first at flows as low as 570 lb h, and additional ones clear as flow is increased.

Run number 233, Figure 13, shows results of a test in which the bundle was blown out, the flow reduced to the minimum blowout flow of 1250 lb h, and the percent moisture increased to between 10 and 20 percent.

These conditions were maintained for 45 minutes adn then all flow was shut off. It took in excess of 15 minutes to reflood the tubes, indicating that even very wet steam at 1250 lb h will keep the bundle clear of water, and that water build-up is prevented.

Figure 14 is a similar run in which, after blowing out, the flow was reduced to the minimum required (700 lb h) to keep the bundle clear. The wetness of the steam was increased to about 20 percent. It is seen that while flow existed, the bundle was kept clear, but upon stopping the flow one of the three instrumented tubes immediately flooded. (Others may also have flooded, but this is not known since only three were instrumented.) In any event, instantaneous flooding of the entire bundle did not occur since two of the three instrumented tubes took several minutes to flood. Thus, it can be concluded that with 700 lb h flowing in a unflooded bundle, the amount of water buildup which can occur is not enough to cause sudden flooding of all the tubes upon loss of flow.

D. Flow Distribution

Flow distribution was measured in the three types of bundle tubes (A, B, and C on Figure 1) by three Pitot tubes mounted in the outlet end of the fuel up-pass.

1. Impact Tube Calibration

The impact tubes were tested in an air system, prior to installation, to ascertain their relative characteristics. It is shown in Figure 15 that the three Pitot tubes agree, within 1-1/2 percent, up to air velocities of 300 ft sec, and are probably within 1 percent when allowance is made for the change in flow distribution across the test pipe outlet. This accuracy was sufficient for the purpose of comparing flows in the fuel bundle tubes.

2. Analysis

The equation for the Pitot tubes is

$$R = K\rho \frac{V^2}{2g_c} , \qquad (4)$$

where R is the differential reading of static and impact pressures.

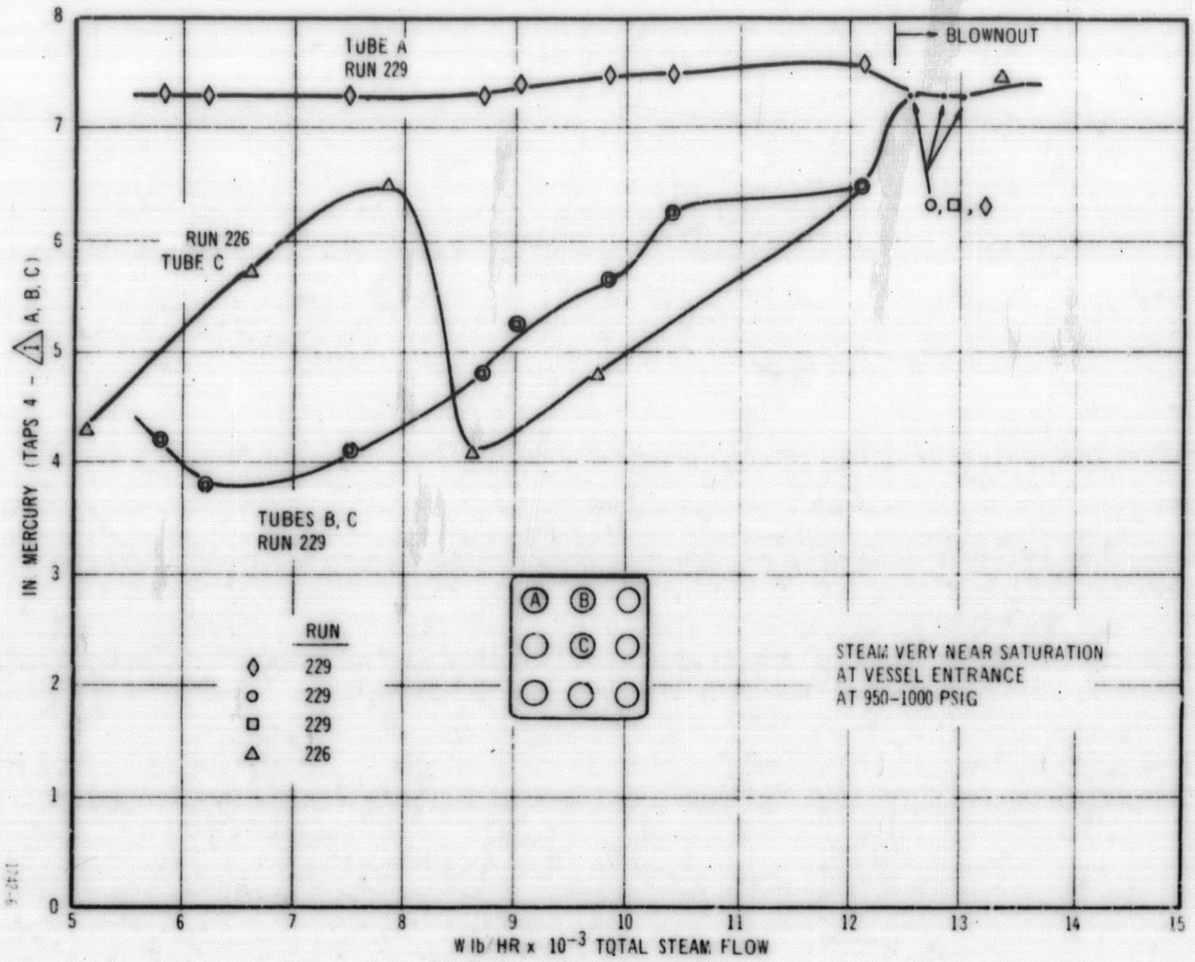

Figure 12. Blowout vs Flow

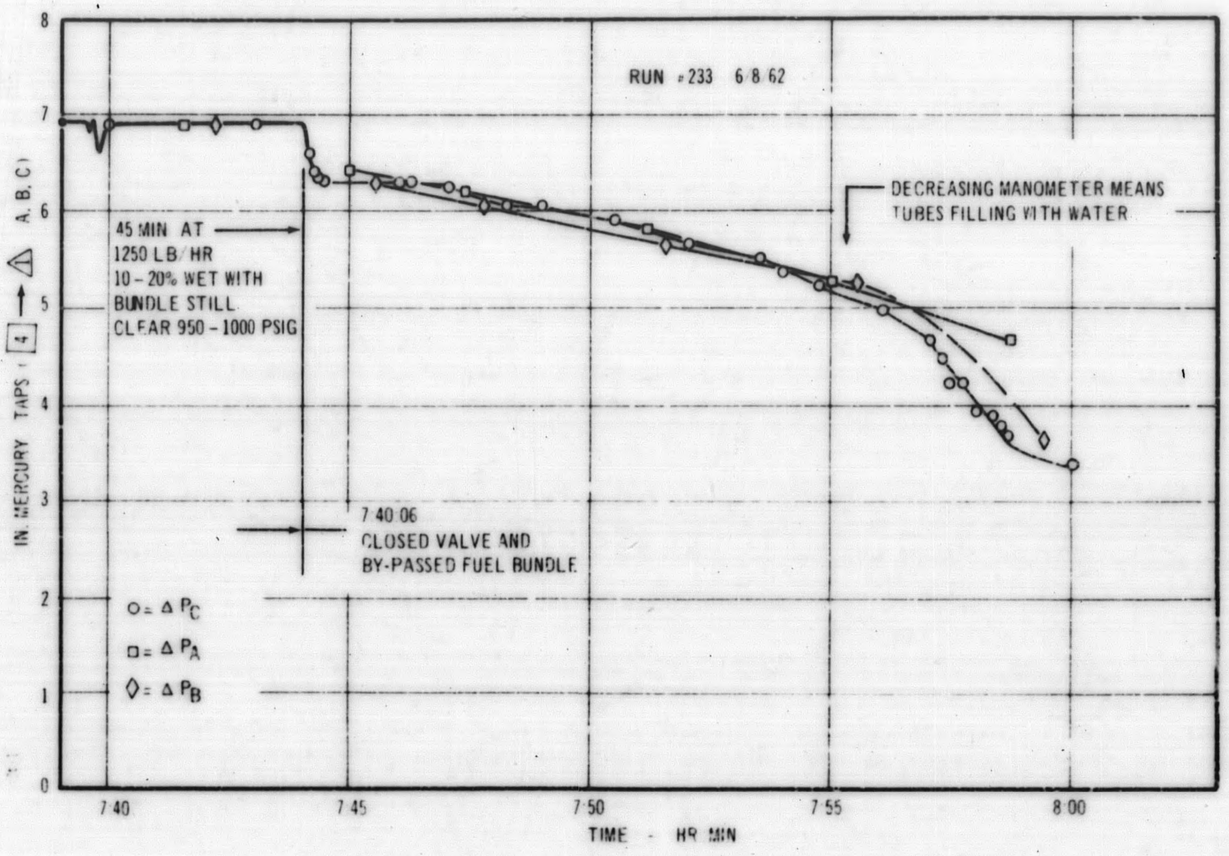

Figure 13. Effect of Wet Steam at Minimum Blowout Flow (1250 lb/h)

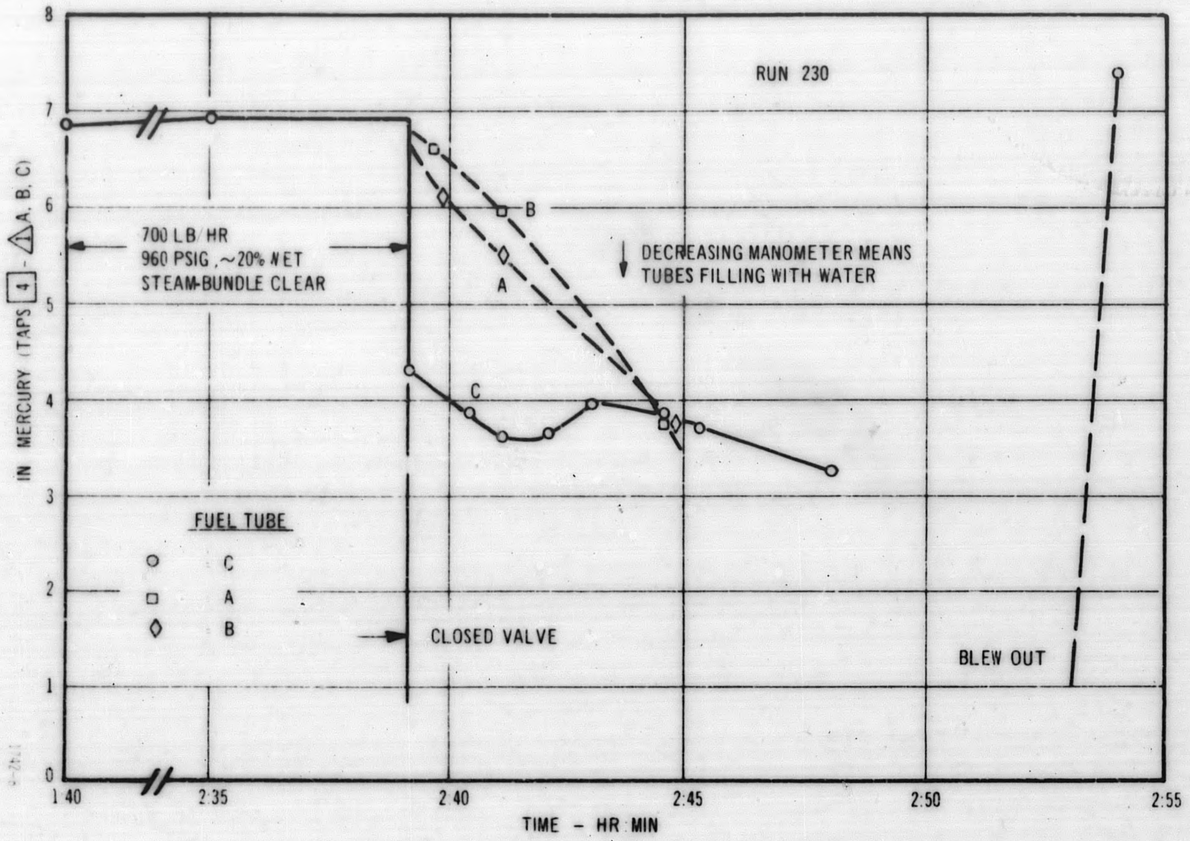

Figure 14. Effect of Wet Steam at Minimum Flow (750 lb/h) after Blowout

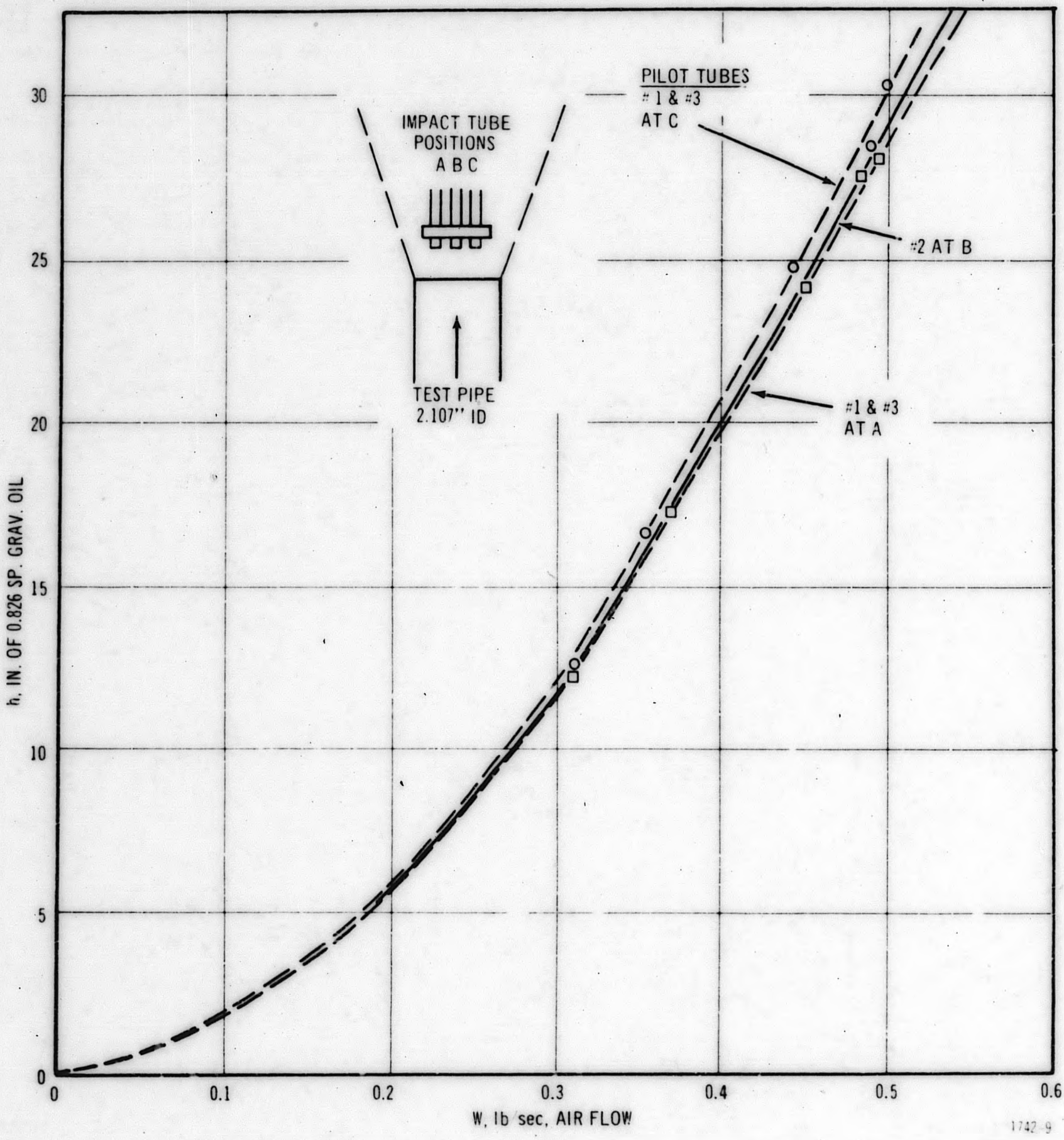

Figure 15. Impact Tube Comparisons

With K the same for the three Pitot tubes, and ρ the same for the three fuel tubes,

$$\frac{W_c}{W_A}\sqrt{\frac{R_c}{R_A}} \quad \text{and} \quad \frac{W_c}{W_B}\sqrt{\frac{R_c}{R_B}}. \tag{5}$$

where subscripts refer to the fuel process tubes.

Then

$$W_T = W_c\left[4 + \frac{1}{\sqrt{R_c R_A}} + \frac{1}{\sqrt{R_c R_B}}\right]. \tag{6}$$

where W_T is the known total flow. From Equations (5) and (6) the flows in the three tubes may be calculated. The latter may then be compared to an equal flow distribution of W_T 9.

3. Test Description

Impact tube readings, taps 12 and 13, were taken when a given steady flow of steam was established through the entire system. These were taken during runs with superheated steam throughout the fuel circuit to ensure reliable head corrections, on the sensing lines of the Pitot tube, inside the vessel. The sensing lines outside the vessel were filled with pressurized water at room temperature.

4. Data Reduction

The physical arrangement of pressure tap lines 12 and 13, Figures 1 and 5, resulted in the following equations for reduction of Pitot tube readings.

Fuel Tubes A, B, and C:

$$R_A = 1728\ \Delta P_{12\text{-}13} = 21.25\,\rho_s + \rho_w\left[M_A\left(\frac{\rho_m}{\rho_w} - 1\right) - 20.25\right] \tag{7}$$

$$R_B = 1728\ \Delta P_{12\text{-}13} = \rho_s + \rho_w\left[M_B\left(\frac{\rho_m}{\rho_w} - 1\right)\right] \tag{8}$$

$$R_C = 1728\ \Delta P_{12\text{-}13} = 4.625\,\rho_s + \rho_w\left[M_c\left(\frac{\rho_m}{\rho_w} - 1\right) - 3.625\right]. \tag{9}$$

R = 1728 (psi), differential reading at sensing location;

ρ_s = lb/ft^3, steam density at Pitot tubes;

ρ_w = lb/ft^3, water in lines outside vessel;

M = Inches, manometer; and

ρ_m/ρ_w = Specific gravity of manometer oil from reference (2).

4. Results and Discussion

Results of the four runs which yielded reliable data are shown in the last three columns of Table III Tube B, the side tube of the bundle, was consistently above the average equally distributed flow. Tubes A (corner) and C (center) were consistently low, with about the same flow in each. The spread in the flow variation among tubes is not sufficient to indicate a trend with flow, and the average values shown should be indicative for the flow range of 4000 to 10, 000 lb/h.

Only four runs were reduced as the data after August 28 was very erratic and indicated some trouble in the system. Disassembly showed that the fins which held the Pitot tubes centered in the fuel tube outlet, had broken. This apparently caused some of the tubes to warp to the side of the fuel tubes and read much lower velocities than the peak intended.

E. Heat Transfer

As described in Section IV, the purpose of the heat transfer tests is to obtain data on the effective heat conductance across the gap in the riser, Figures 1 and 16.

1. Test Description

Steam was directed through the fuel in the "reverse" direction, as shown in Figure 2, to simulate a positive temperature gradient radially outward through the gap, as obtained in the normal operating flow direction. The vessel was brought up to temperature and pressure with a low flow of about 2000 to 3000 lb/h at 1000 psi. The desired test flow, and full water level of 18 to 19 ft, was established and temperatures allowed to stabilize. The latter was ascertained on a Brown Recorder, which showed all thermocouples, and stabilization of temperatures occurred in a few minutes.

The temperature recorder charts were marked at the start and end of runs. As the run progressed the water level dropped, very rapidly at high flows when heat transfer was high, and water level readings recorded on the temperature charts. Flow conditions and pressures were recorded to complete the run.

The water level was then raised, flow reset, and a new run started when conditions were stable.

TABLE III

RELATIVE FLOWS IN THREE UNIQUE FUEL BUNDLE TUBES

Date (1962)	Run Number Date	W lb/h Total $\times 10^{-3}$	P_{20} psia	°F Steam at Pitot Tubes	Manometer and Specific Gravity of Fluid (Red Oil)				R, psi			W_C lb/h $\times 10^{-3}$	Ratio Measured Flow to Equal Flow Distribution		
					A	B	C	$\frac{\rho_m}{\rho_w}$	A	B	C		A Corner	B Side	C Center
5 24	220	10.17	1012	588	33.1	29.7	26.8	2.958	2827	3637	3062	1.105	0.94	1.07	0.98
8 27	234	5.68	1015	653	15.92	9.7	9.17	2.962	724	1191	906.1	0.618	0.88	1.12	0.98
8 28	235	6.51	1013	665	22.70	14.01	13.17	2.951	1537	1707	1385	0.675	0.98	1.03	0.93
8 28	236	4.78	1014	658	12.40	6.50	6.27	2.967	295.9	800.8	552.3	0.511	0.95	1.05	0.96
					14.40	5.34			541.8	658.2	Averages		0.94	1.04	0.96

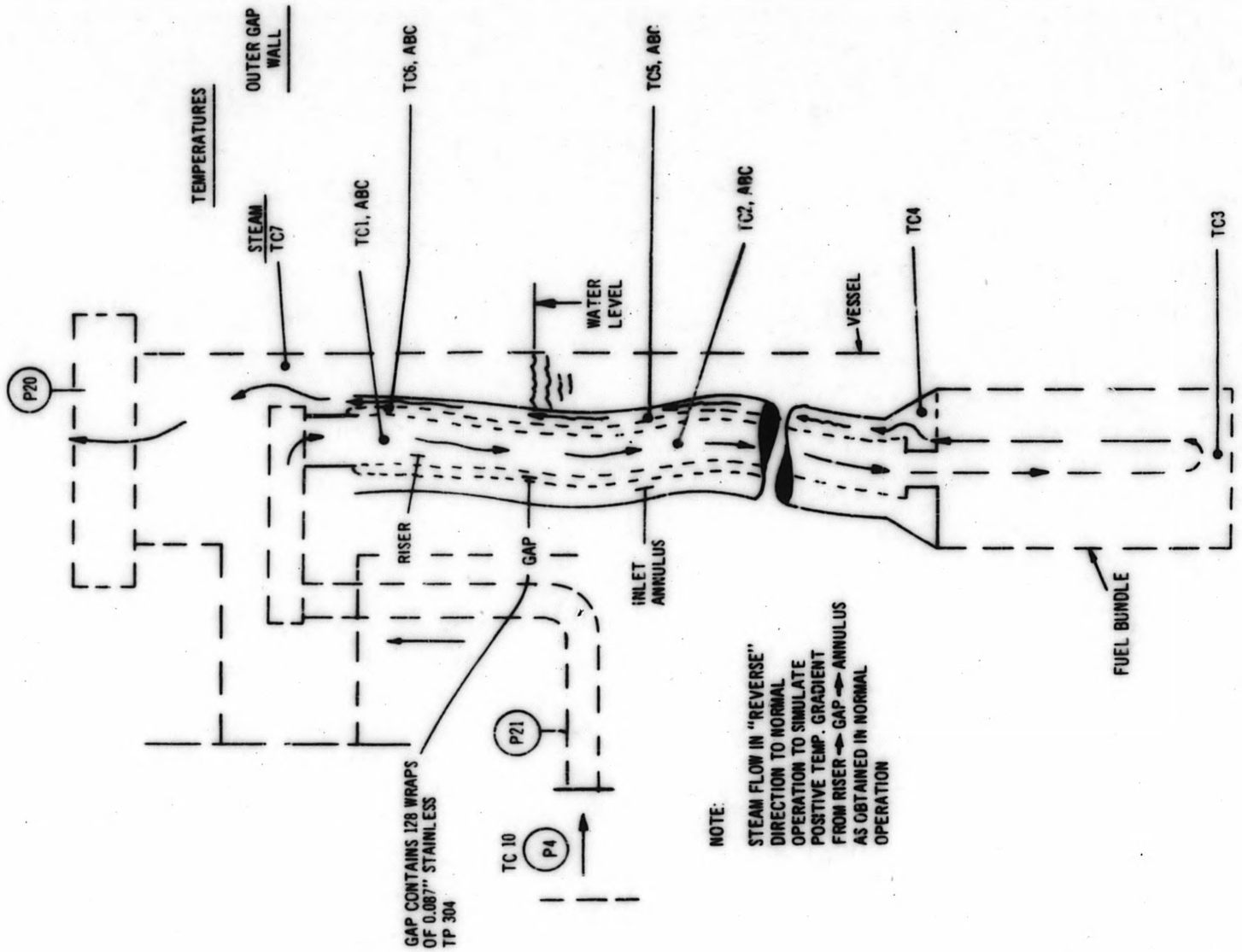

Figure 16. Schematic of Flow and Temperature Locations in EVESR MKI Fuel Bundle

2. Analysis

The heat transfer through the steam gap, Figures 17 and 18, is calculated on the basis that the gap contains steam only. This will be compared to the measured heat transfer through the gap which contains spiral wire wrapping. In addition, expansion gaps permit steam circulation along the length of the gap.

The radial heat transfer from the riser to the annulus, is given by

$$T_i - T_o = \frac{q_L\left(\frac{Btu}{h\text{-}ft}\right)}{2\pi}\left[\frac{\ln\frac{R_2}{R_1}}{k_1} + \frac{\ln\frac{R_3}{R_2}}{k_s} + \frac{\ln\frac{R_4}{R_3}}{k_3}\right]. \tag{10}$$

For the dimensions shown

$$T_i - T_o = \frac{q_L}{2\pi}\left[\frac{0.0816}{k_1} + \frac{0.0867}{k_3} + \frac{0.0997}{k_s}\right]. \tag{11}$$

The temperature drops through the steel walls are very small compared to that through the steam gap ($k_{1,3} \sim 10.$ and $k_s \sim 0.03$).

The temperature drop through the steel walls can be neglected with little error - about 0.016 in 3 or less than 1 percent - and

$$q_L = \frac{dq}{dL} = \frac{2\pi k_s}{0.0997}(T_i - T_o) = 62.9\, k_s\,(T_i\, T_o), \tag{12}$$

The thermal conductivity of the steam in the range tested (600 to 800°F) is

$$k_s = 0.0241 + \frac{0.00373}{10^2}(T_s - 400). \tag{13}$$

The calculation of the total q along the entire length in Equation (12) is simplified by assuming linear, radial, and longitudinal temperature variations. This is not strictly true but is justified for the comparison of heat transfer with and without wire in the gap. It will be seen later that the wire wrap increases the heat transfer on the order of 10 to 20 times. Then

$$T_i = T_{1w} - \frac{T_{1w} - T_{2w}}{L_t}\, L, \tag{14}$$

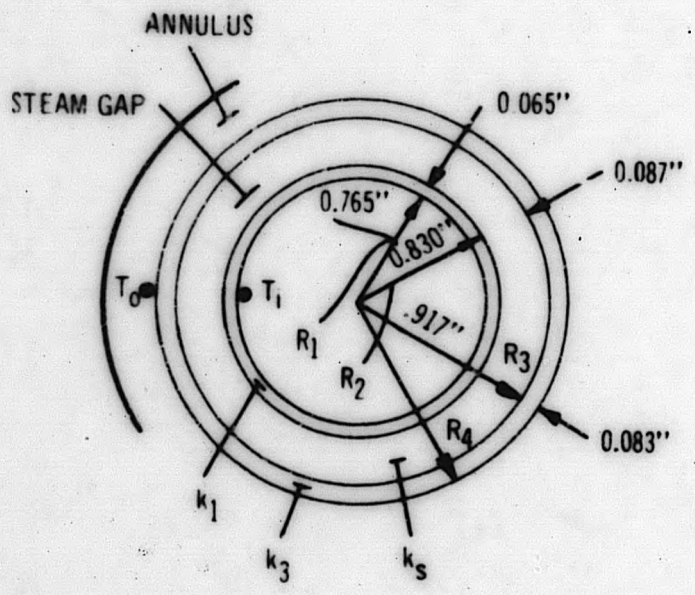

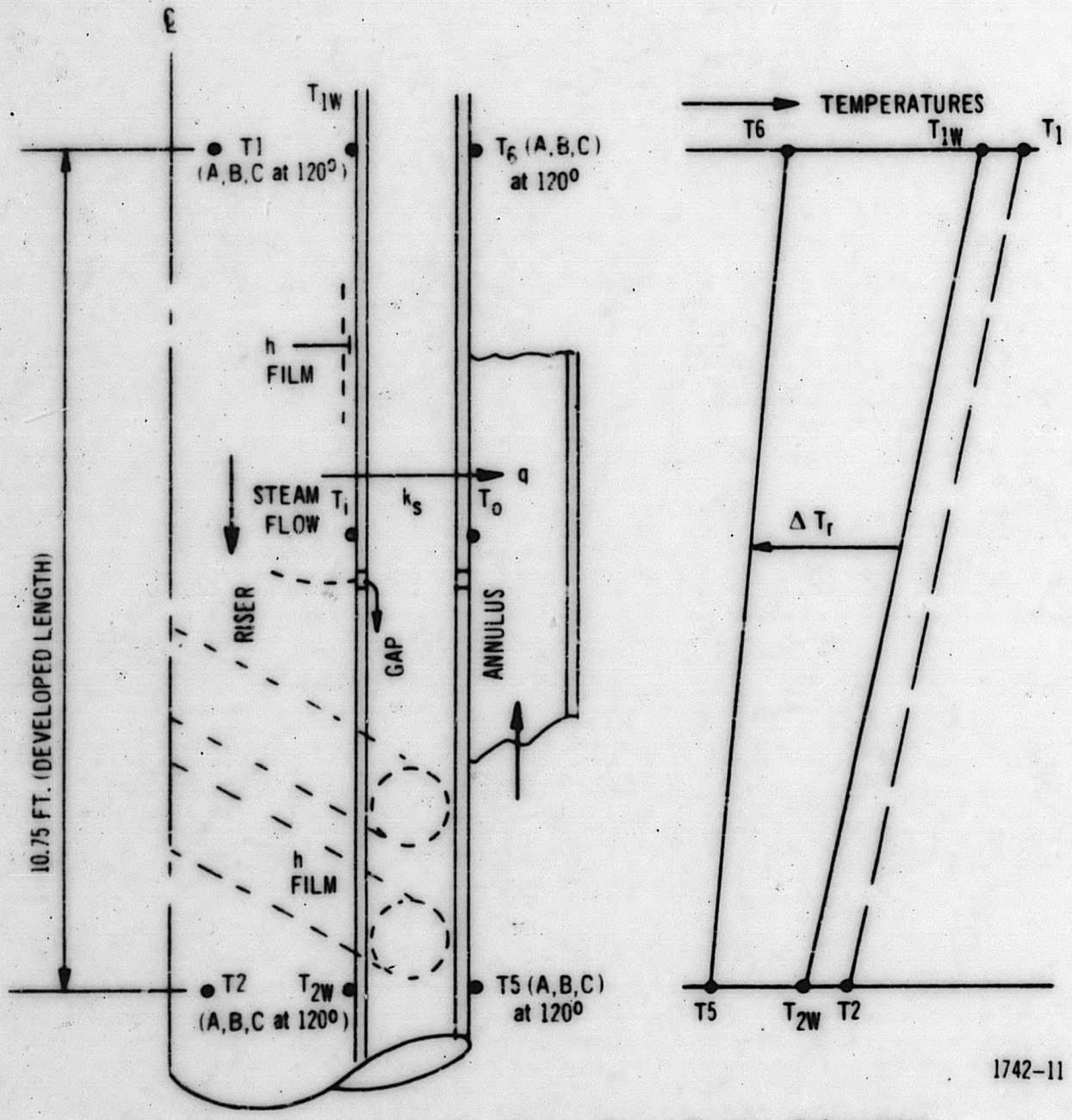

Figure 17. Riser Cross Section Schematic

$$T_i - T_o = \Delta T_{r1} - \frac{\Delta T_{r1} - \Delta T_{r2}}{L_t} L, \tag{15}$$

where

$$\Delta T_{r1} = T_{1w} - T_6, \text{ and}$$

$$\Delta T_{r2} = T_{2w} - T_5.$$

Also,

$$T_5 = T_i + \frac{\Delta T_r}{2}. \tag{16}$$

Then in Equation (12)

$$k_s = 0.0092 + \frac{0.00373}{100}\left[T_{1w} + \frac{\Delta T_{r1}}{2} - \left(\frac{\Delta T_{Lw}}{L_t} + \frac{\Delta\Delta T_r}{2L_t}\right)L\right], \tag{17}$$

with

$$\Delta T_{Lw} = T_{1w} - T_{2w}$$

and

$$\Delta\Delta T_r = \Delta T_{r1} - \Delta T_{r2} = T_{1w} - T_6 - (T_{2w} - T_5).$$

Substituting Equations (15) and (17) into Equation (12), integrating and simplifying results in the average heat loss per foot for a stagnant steam annulus,

$$\frac{q\left(\frac{Btu}{h}\right)}{L_t} = \left(0.289 + 0.117\,\frac{T_{1w}}{100} - 0.039\,\frac{\Delta T_{Lw}}{100} + 0.0392\,\frac{\Delta T_{r1}}{100}\right)(\Delta T_{r1} + \Delta T_{r2}) +$$

$$0.039\,\frac{\Delta T_{r2}}{100}\,(\Delta T_{r2} - \Delta T_{Lw}). \tag{18}$$

The heat transfer coefficient in the riser was taken constant along the length and calculated from the Dittus-Boelter equation,

$$\frac{h}{10^3} = 25.7\, k_1 \left(\frac{w/10^3}{\mu_1}\right)^{0.8} \left(\frac{c_p \mu}{k}\right)_1^{0.33}, \tag{19}$$

where

1 = steam at TC1 conditions,

w = lb/h,

μ = lb/h-ft.

Total heat transferred was

$$q = W(H_1 - H_2); \tag{20}$$

H = Btu/lb enthalpies at TC1 and 2.

3. Effect of Wire Wrap on Gap Conductivity

The steam gap, Figure 16, contains 128 wraps of 0.087-inch stainless wire or a full length of 11.14 inches of round wire.

If p is the length of wire in "solid contact" in the annulus of length L, so there are two paths in parallel, then the effective conductivity of the gap may be estimated as

$$\frac{k_{eff}}{k_s} = 1 + \frac{p}{L}\left(\frac{k}{k_s} - 1\right), \tag{21}$$

and approximately for the entire annulus

$$q_{ACTUAL} = k_{eff}\, q_s. \tag{22}$$

where

k = Btu/h-ft-°F, for steel wrapping, and

k_s = Btu/h-ft-°F, for steam.

The value of q_s is calculated as above [Equation (18)] for a stagnant steam annulus.

4. Data Reduction

Heat loss in the riser was calculated by Equation (20) and an average film drop in the riser calculated using the h from Equation (19). This was used to calculate the inner riser wall

temperatures, T_{1w} and T_{2w} and ΔT_{Lw}. The total heat loss for a stagnant steam annulus was then calculated by Equation (18) for comparison to the actual annulus with wire wrapping and openings which allow steam circulation.

Allowance was made for pressure drops in obtaining the enthalpy at TC2. The thermocouple calibrations showed them to be so close, that the deviations cancel (or there is negligible error) for temperature differences. Thus, the temperatures shown in Table IV are uncorrected.

5. Results and Discussion

The principal results are shown in Tables IV and V. The flows and various temperature readings are shown in Table IV; the calculated results for film coefficient in the riser, total heat transfer, radical and longitudinal temperature differences, and the ratio of measured to calculated [Equation (18)] average heat transfer per foot are shown in Table V.

The radial temperature differences are plotted versus flow on Figure 19. The trend of decreasing radial temperature differences, with increasing flow, is fairly well established. This is consistent with the higher rates of heat transfer expected at higher flows, at lower radial temperature differences. Two curves at two different ranges of inlet steam temperature are shown in Figure 24. The ordinate may be rearranged to give $(T_1-T_2) - (T_6-T_5)$, so the curves reflect a temperature difference that is approximately proportional to the temperature loss of the incoming steam and the temperature rise of the exit steam. This difference should become smaller as flow increases.

The increase of heat transfer across the gap with flow is plotted on Figure 20.

The average increase from 2000 to 8000 lb/h is about 2-1/2, which is roughly comparable to a value of 3 that would be predicted by the 0.8 power of the flow ratio.

There is considerable scatter in the data and no definite trend apparent with change in vessel water level or the temperature level of the inlet steam.

A mean line is drawn through the data which is a good representation to about ±30 percent if two or three of the extreme points are ignored. Part of the scatter is probably due to different degrees of contact resistance, due to expansion and contraction between the wire wrap and the steam, to which the heat transfer rate is quite sensitive (see below).

A mean line through most of the data is

$$\frac{q_{MEASURED}}{q_{STAGNANT\ STEAM}} = 11.5 + 1.69\ \frac{W_{lb/h}}{10^3} \qquad (23)$$

TABLE IV

TEMPERATURE DATA FOR HEAT TRANSFER RUNS

Run Number	$\frac{W}{10^3}$ lb/h	P_{20} psia	Liquid Level LL ft-in.	TC1[1] Average	TC2 Average	TC3 Bottom Fuel STM	TC4 Enter Annulus Bottom STM	TC5 Average	TC6 Average	TC7 Out Annulus Top Vessel
250	2.14	1012	18-10	749.5	722.5	676	607.5	597.5	591	585.5
		1015	17-8	749.5	722	675	598.5	595.5	590.5	585
		1017	16-6	750.5	722.5	676.5	600	596.5	591.5	585
		1018	15-4	750.5	723.5	677.5	599	593	591.3	585.5
249	2.10									
251	2.14		18-10			673	600			585
252	2.94		18-10			679.5	602.5			585
253	2.98	1014	18-10	736	717	677.5	616	597.5	590.5	585.5
		1013	17-8	736.3	719	678.5	605	597.5	591.5	585.5
		1015	16-6	737.8	719.2	680	616	600	595	590.5
		1010	15-4	737.8	718.3	680	610.5	599.3	595	592
254	4.79									
255	4.86	1015	18-10	769.5	752.2	691	622.5	622.5	613.8	614
			17-8	775.3	756.2	697	626	622.5	615.5	612
		1017	15-11	778.5	754.7	697	625	622.5	619	617
			15-4	778	759.5	696.5	625	622.5	618.7	617
256	4.85									
257	4.84	1016	18-10	770.8	753	690	627	622	614	615
		1017	17-8	771.2	753.8	689	622.5	620.3	616.5	618
		1017	16-6	771.2	753.8	693	627	620.3	617.3	617.5
		1016	15-4	771.7	754	688	621	619.5	613	625
258										
259	5.61		18-10	754.5	731.7	683	606.5	623.8	612	610
		1015	16-6	781	764.2	707	631	618.5	608	607
		1016	17-8	764	751.5	714.5	624	622.3	614.3	614.5
			15-4	788	768	723	636	628.5	624.3	621.3
260	6.75		18-10	776.8	760.8	704	618	618.3	616	607
		1015	17-8	781.5	764.5	714.5	617.5	618	615	609.5

[1] All Temperatures are F

TABLE IV (Continued)

Run Number	W / 10^3 lb/h	P_{20} psia	Liquid Level LL ft-in.	TC1[1] Average	TC2 Average	TC3 Bottom Fuel STM	TC4 Enter Annulus Bottom STM	TC5 Average	TC6 Average	TC7 Out Annulus Top Vessel
260 (Cont'd)	6.75		15-11	787.5	772.2	726	628	628.8	622	618
			15-4	791.2	774	727	628	627.7	625.7	620
261										
262	6.76									
263	7.39	1011	18-10	693.5	683.2	659	620.5	615	608.7	609
		1013	17-8	684	678.7	661	610.5	610	606.5	611
		1012	15-11	677.2	672.5	650	616.5	610.5	606	609.5
		1010	15-4	672.7	666.7	647.5	609.5	602.3	602	610.5
264	6.13									
265	5.19	1015	18-10	678.7	673.5	657	616	609.8	604.7	595.5
		1013	17-8	679.2	673	657	611.5	605.7	603.8	596
			16-6	684	673.5	657	617	608	605.5	596.5
			15-4	688.5	680.5	663.5	621.5	612.5	611.5	601.5
247										
248										

[1] All Temperatures are °F

TABLE V

TEMPERATURES AND HEAT TRANSFER DATA

Run Number	Liquid Level in Vessel ft	Btu/h-ft^2°F Riser Film	$q/10^3$ Total Btu h Transferred	T_{1w}	T_{2w}	ΔT_{r1}	ΔT_{r2}	$\frac{q}{L}$ Calculated	$\frac{q}{L}$ Measured Btu h-ft	$\frac{q \text{ Measured}}{q \text{ Calculated}}$
250		188	37.66	703.5	676.1	112.4	80.5	222.7	3500	15.8
253		244	36.06	702.6	684.1	109.6	85.5	226.2	3350	14.8
255	18'-10"	362	54.43	730.5	713.2	116.7	90.7	247.6	5060	20.4
	17'-8"		58.81	736.3	717.2	120.8	94.7	259.9	5460	21.1
	16'-6"		73.39	739.5	715.7	120.5	93.2	257.5	6810	26.4
	15'-4"		56.86	739	720.5	120.3	98	261.4	5280	20.2
257		362	54.21	736.5	719.0	121.3	98.5	265.6	5040	19.0
259	(1)	406						180.5	7670	
								309.2	5490	
								276.0	4230	
			82.47	707.5	684.7	95.5	60.9	270.5	6630	37.1
			45.44	738.1	725.6	123.3	103.3	245.5	5230	17.2
			58.91	747.3	130.5	139.3	112.0	300.2	5490	18.3
			71.25	747.3	727.3	123.0	98.8	281.8	6630	23.5
260	(1)	472	67.00	743.8	727.8	127.8	109.5	290.2	6220	21.4
				748.5	731.5	133.5	113.5	303.9	6470	21.3
				754.5	939.2	132.5	110.4	300.4	5780	19.3
61				758.2	741.0	132.5	113.3	305.1	7470	21.2
263	(1)	523	51.73	679.0	668.7	70.3	53.7	138.4	4810	34.7
			25.87	669.5	664.2	63.0	54.2	129.6	2410	18.6
			23.65	662.7	658.0	56.7	47.5	114.1	2200	19.3
			29.56	658.2	652.2	56.2	49.9	115.5	2750	23.8
265	(1)	396	26 47	663.2	658.0	58.5	58.2	116.9	1545	13.2
				663.7	657.5	59.9	51.8	122.6	2120	17.3
				668.5	658.0	63.0	50.0	124.4	3570	28.7
				673.0	665.0	61.5	52.5	126.3	2710	21.4

(1) Liquid levels same as Run 255 in order shown

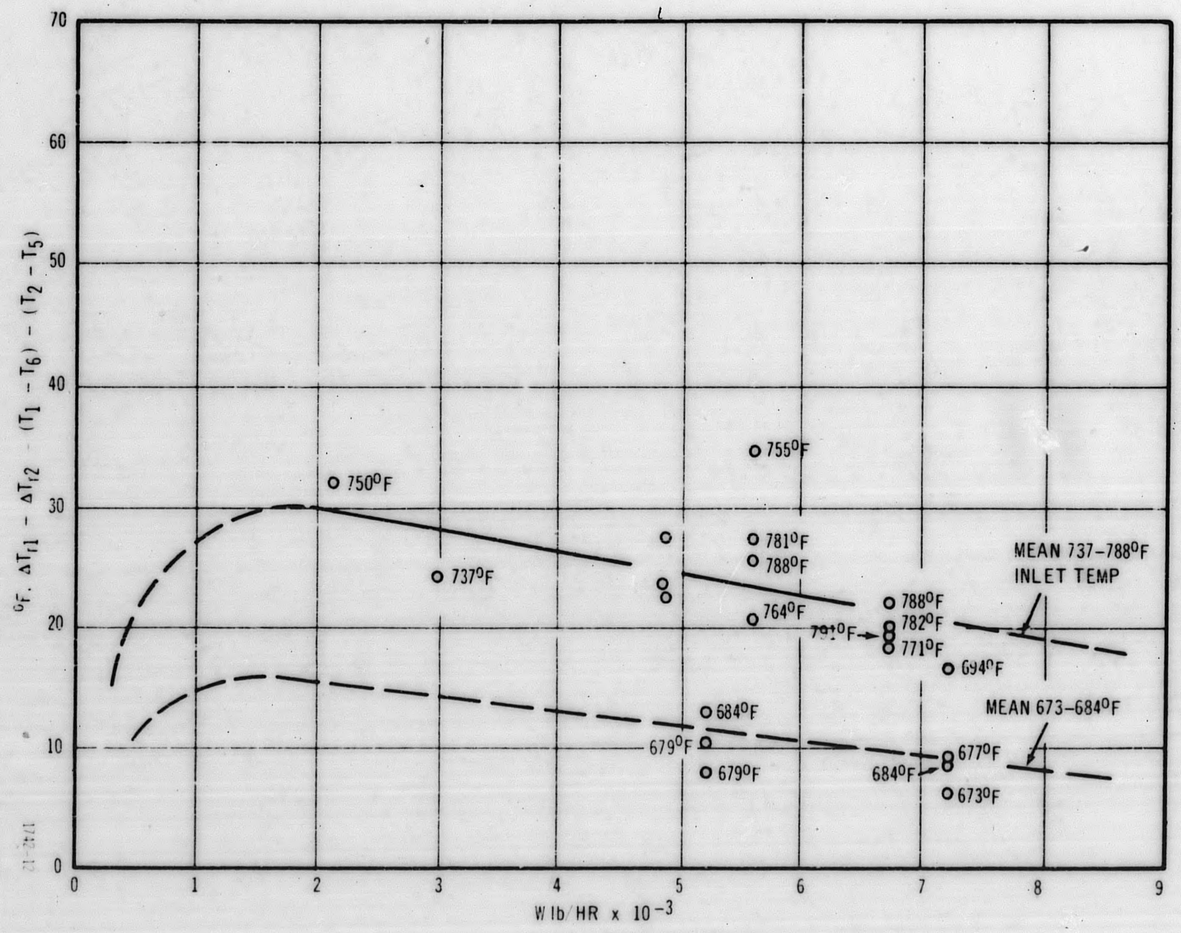

Figure 19. Effect of Flow on Radial Temperature Differences Across Steam Gap

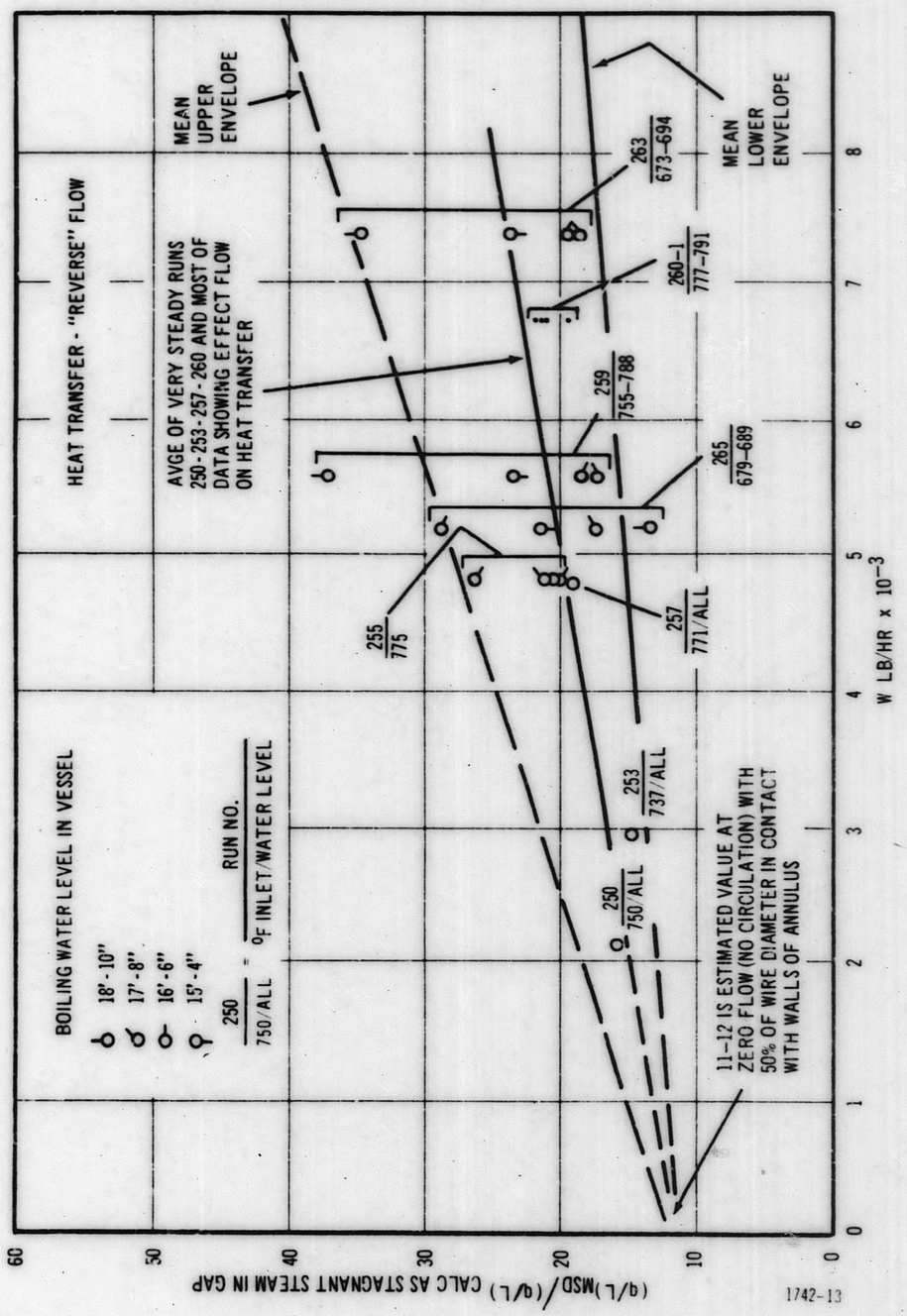

Figure 20. Effect of Flow on Heat Transfer Rate, Riser to Annulus

This line is extrapolated to a value of about 12 at zero flow. This value makes possible an estimate of the effect of wire wrapping on the effective conductivity of the stagnant annulus.

Figure 21 shows a line for fractional length of wire wrapping in "solid" contact with the walls of a riser length L. The conductivity increases very rapidly for small fractions of steel length. For the ratio of 12 obtained above, measured calculated stagnant annulus, 4 percent of the riser length is estimated as steel in solid or perfect contact. This is 0.04 (11.75 feet of riser length) or 5.6 inches/11.1 inches wire, which equals about 50 percent of the wire diameter in good contact with the gap walls. This appears to be a reasonable value.

If the value of 50 percent wire contact is accepted, the increased calculated heat transfer rates on Figure 20 may be attributed to flow. As shown above, this is also a reasonable check with the 0.8 power of the flow. The mean line shown varies as the 0.67 power of the flow.

F. Pressure Drop

1. Test Description

The fuel bundle and riser were extensively instrumented with pressure taps to allow measurement of the pressure losses through the various components. Some of the passages are of elaborate design and experimental values are required for reliable data and for bases in future designs and modifications.

Steady-state flow of superheated steam, with various inlet temperatures, was established in the normal flow direction, and pressure differences were measured from selected reference taps (see Figure 22) to various other points in the system. A high-pressure manometer, with mercury or red or blue Merriam fluid, was used for most of the runs. When the manometer leg of 60 inches of mercury was exceeded for high flow runs, the Heise gage, P20, was used to measure static pressures directly. In some cases, two or three reference taps were used with the manometer to cover all of the taps along the flow circuit.

Usually, the temperatures at vessel inlet, fuel inlet, bottom of fuel, fuel exit, and vessel exit were read. From these, a mean temperature in each of the passages of the circuit could be calculated for evaluation of mean density in the passage.

It was physically impractical to locate seal pots right at the exit from the vessel. Thus, it was necessary to exercise care to ensure that pressure taps, exterior to the vessel, were at ambient temperature so static head corrections could be evaluated properly.

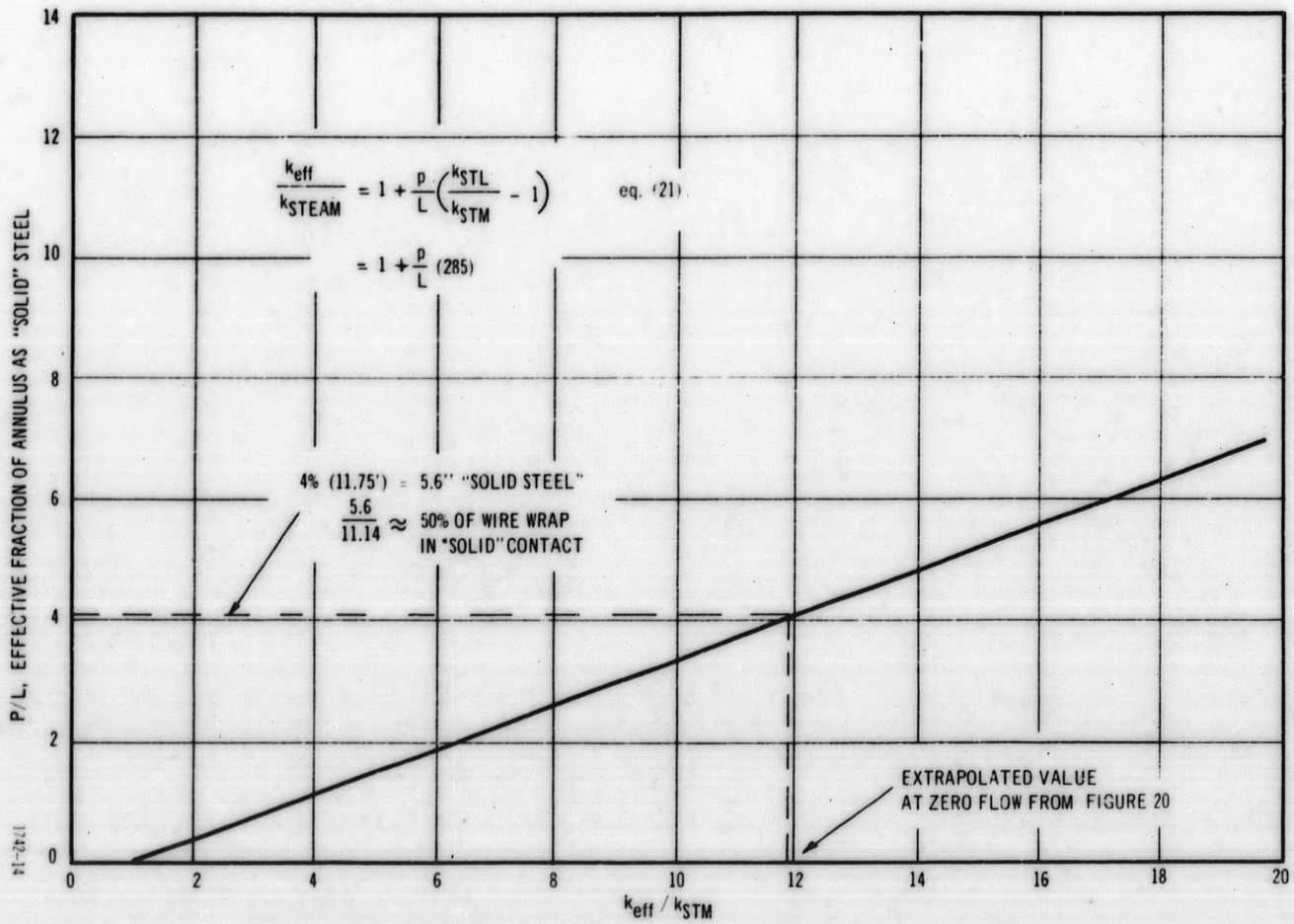

Figure 21. Estimated Fraction Wire Wrap in Contact with Annulus Walls

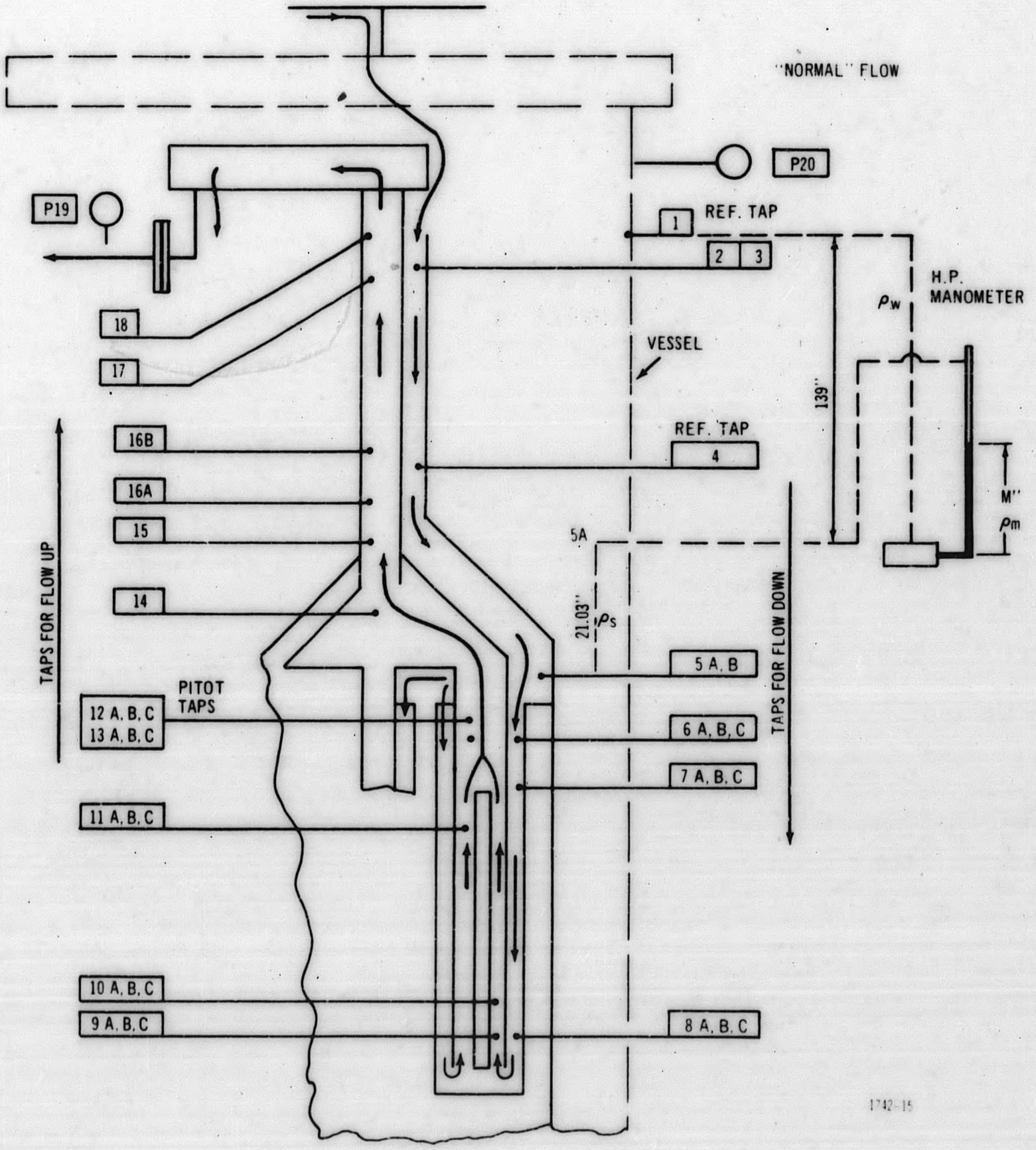

Figure 22. Schematic of Pressure Tap Numbers and Location

Occasionally a full manometer swing would warm up part of a line leading to the seal pots, and it was necessary to allow the line to cool to ambient temperature.

2. Data Reduction

Figure 22 shows the pressure tap numbers and their location in the flow circuit. The left side of Figure 5 shows the elevation dimensions for the sensing element of a pressure tap, and the right side the elevation at which the tap exits from the vessel and thereafter is at system pressure and ambient temperature.

3. Static Pressures

Static pressures in the circuit were obtained from a pressure balance in the manometer. A typical case, for tap 5A in Figure 22 is

$$p_1 + (139 + M)\rho_w = p_{5A} - 21.03\,\rho_s + M\rho_m, \text{ and}$$

$$p_1 - p_{5A} = \rho\frac{w}{1728}\left[M\left(\frac{\rho_m}{\rho_w} - 1\right) - 139\right] - 0.0122\,\rho_s, \text{ with} \qquad (24)$$

p = psi, static pressure;

ρ_w = lb/ft^3, density, water at ambient temperature and system pressure;

ρ_s = lb/ft^3, steam at temperature of inlet steam which surrounds the lines in the vessel, and estimated pressure at the tap;

M = Inches, manometer; and

$\frac{\rho_m}{\rho_w}$ = Specific gravity of manometer fluid at ambient temperature

NOTE Compressibilities of the manometer fluid and water are assumed the same and will cancel.

Static pressure differences between various taps were then obtained by differences from Equation (24), e.g.,

$$p_{5A} - p_{7A} = (p_1 - p_{7A}) - (p_1 - p_{5A}). \qquad (25)$$

4. Frictional Loss in Fuel Passes

The standard mechanical energy balance was used for frictional pressure losses

$$p_1\,\bar{v}_1 + \frac{V_1^2}{2g_c} + z_1 = p_2 v_2 + \frac{V_2^2}{2g_c} + z_2 + \Delta p_f \bar{v} + \Delta p_{ce}\bar{v}, \qquad (26)$$

v = ft^3 lb;

z_1 = ft, height above datum;

p = lb ft^2, pressure;

L = ft, length; and

friction loss with commonly used nomenclature is

$$\Delta p_f = \frac{f_M L}{2g_c D_h A^2} (w^2 v). \quad (27)$$

Contraction or expansion losses were calculated from

$$\Delta p_{c,e} = \frac{K}{2g_c A^2} (w^2 v). \quad (28)$$

5. Correlation of Total Pressure Drops for Runs at High Variation of Temperature, Pressure and Specific Volume

It was desirable to reduce all of the total frictional pressure drops, made at various temperatures and pressures, to a common temperature for comparison and check on consistency. Then the mean ft^3 lb could be determined at that "base" temperature and the mean pressure in the particular component. For most runs up to 10,000 lb h, variation of ft^3 lb in a pass was relatively small so the average, v, value was usually within a few percent. The following method was used for normalizing total frictional pressure drop:

a. Assuming $f_M = \frac{c}{(Re)^m}$:

$$\Delta p_f \propto c\, w^{2-m}\, v\, \mu^m. \quad (29)$$

For the temperature range of 550 to 800°F tested at 1000 psi, a maximum variation of $\mu^{0.25}$ is +4/-3 percent so effect of viscosity was neglected. This would cause an error on the order of only ±1 percent at the lower temperature variations tested.

b. Constant Temperature Runs.

From several runs, at almost constant temperature, the percentage pressure drop in each of the main flow segments was found to remain essentially constant as indicated in Table VI.

TABLE VI

AVERAGE Δp, psi, DATA FROM FSSENTIALLY CONSTANT TEMPERATURE RUNS

Run	w lb h $\cdot 10^{-3}$	Inlet Annulus Taps 1-5		Fuel Pass Taps 5-14		Riser and Outlet Taps 14-19	
		Δp	Percent Total	Δp	Percent Total	Δp	Percent Total
246	3.19	1.04	12	6.48	75	1.12	13
239	5.68	2.98	14	16.33	76	2.31	10
236	4.21	1.60	12	10.46	76	1.64	12
235	6.51	3.90	13	22.81	77	3.02	10
270	13.37	13.6	10	108	77	18.0	13
	Average Percent		12		76		12

c. By Equation (29), for constant temperature

$$\Delta p_{T\ c} \quad w^{2-m}\, \upsilon_c \sum_{\text{passes}} C, \tag{30}$$

(where C is dependent on geometry of the pass only) for a constant temperature run. At the same mass flow, for variable temperature

$$\Delta p_{T\ V} \quad w^{2-m}\left[C_D \bar{\upsilon}_D + C_F \bar{\upsilon}_F + C_R \bar{\upsilon}_R\right], \tag{31}$$

where the subscripts stand for downcomer, fuel, and riser.

Also, if r is the fractional pressure drop in each pass

$$r_{DC} = \frac{w^{2-m} C_D \bar{\upsilon}_c}{\Delta p_c} = \frac{C_D}{\Sigma C}, \tag{32}$$

$$r_{FC} = \frac{C_F}{\Sigma C}, \text{ and } r_{RC} = \frac{C_R}{\Sigma C}. \tag{32}$$

Then from Equations (30) through (32),

$$\Delta p_{T\ C} = \frac{\bar{\upsilon}_C \Sigma C}{\Sigma C\left[r_D \bar{\upsilon}_D + r_F \bar{\upsilon}_F + r_R \bar{\upsilon}_R\right]} \Delta p_{T\ V}. \tag{33}$$

Substituting the average value of r from Table VI, Equation (33) reduces to

$$\Delta p_T \quad C \quad \frac{v_C}{0.12\,(v_D + v_R) + 0.76\,v_F} \quad \Delta p_T \quad V. \tag{34}$$

d. Conditions of 650 F and 1000 psi were chosen for the reference specific volume v_C for normalization, and comparison of the various data. The $v_{D,R,F}$ are evaluated for the runs at variable temperature and the total pressure drop at a constant temperature of 650 F calculated by Equation (34).

6. Results and Discussion

The component frictional pressure drops, at actual run conditions, were calculated by Equations (25) through (28), and are listed in Table VII. The total frictional pressure drops were normalized by Equation (34), and results are shown in Table VIII.

The data in Tables VII and VIII has been plotted for the principal components of the flow circuit shown in Figure 22.

Figure 23 is a typical static pressure profile, along the flow circuit, which shown relative drops in the different components.

The various frictional pressure losses plotted versus flow or $(w\ 10^3)^2 v$ are shown in the balance of the figures (24 through 32).

The frictional losses have been calculated by Equations (25) through (28).

In one case (Figure 32) the riser-exit loss is shown as a static drop. However, the velocity head change is so small, comparatively, that the frictional and static pressure drops are practically the same.

It should be recalled that the total pressure drop in Figure 24 has been normalized to a constant steam temperature of 650 F at 1000 psi through the flow circuit. This allowed comparison of the various runs for consistency. As may be noted on Figure 24, the various runs correlate within 15 percent, with the over-all loss proportional to almost the square of the velocity. This is compatible with the high fraction of expansion- and contraction-type losses in the total circuit (24 percent of total loss).

TABLE VII

COMPONENT PRESSURE LOSSES (All Δp are in psi)

Run Number	Tap	W lb/h ×10⁻³ / (W/10³)²	Static Δp_{5-7}	$\bar{v}$	Fuel Downpass Friction Δp_{7-8}	$\bar{v}$	Fuel Bottom Turn Friction Δp_{8-10}	$\bar{v}$	Fuel Uppass Friction Δp_{10-11}	$\bar{v}$	Exit Fuel → Start Riser Friction Δp_{11-14}
235	A	6.11 / 37.33	0.951	0.570	3.669	0.580	1.421	0.582	14.889	0.590	1.319
	B	6.11 / 37.33	0.802	0.570	3.868	0.580	0.658	0.582	15.665	0.590	1.256
	C	6.11 / 37.33	1.105	0.570	3.805	0.580	0.921	0.582	15.376	0.590	0.852
108	A	8.47 / 71.74	2.078	0.530	7.278	0.520	4.761	0.535	30.790	0.550	2.616
	B	8.47 / 71.74	2.078	0.530	7.278	0.520	4.761	0.535	30.790	0.550	2.616
	C	8.47 / 71.74	2.078	0.530	7.278	0.520	4.761	0.535	30.790	0.550	2.616
220	A	9.88 / 97.61	1.533	0.510	6.631	0.520	18.116	0.535	29.728	0.550	3.500
	B	9.88 / 97.61	1.523	0.510	6.664	0.520	16.799	0.535	32.225	0.550	2.297
	C	9.88 / 97.61	2.539	0.510	6.556	0.520	17.321	0.535	29.224	0.550	3.868
103	A	10.72 / 114.92	2.775	0.485	11.272	0.485	6.009	0.500	41.170	0.510	8.163
	B	10.72 / 114.92	2.310	0.485	11.237	0.485	3.413	0.500	44.665	0.510	7.764
	C	10.72 / 114.92	3.191	0.485	11.355	0.485	4.511	0.500	42.668	0.510	7.664
269	A	13.37 / 178.76		0.550		0.545	8.764	0.575	72.943	0.605	
	B	13.37 / 178.76		0.550		0.545	9.764	0.575	75.943	0.605	
	C	13.37 / 178.76		0.550		0.545	9.764	0.575	73.943	0.605	
270	A	13.37 / 178.76	5.300	0.550	16.162	0.555	1.595	0.580	75.943	0.605	6.603
	B	13.37 / 178.76	3.800	0.550	15.662	0.555	0.595	0.580	73.943	0.605	11.603
	C	13.37 / 178.76	5.700	0.550	15.762	0.555	4.595	0.580	70.943	0.605	8.603
109	A	13.37 / 178.76	4.285	0.565	19.083	0.575	7.467	0.585	21.323	0.590	11.281
	B	13.37 / 178.76	4.285	0.565	19.083	0.575	7.467	0.585	21.323	0.590	11.281
	C	13.37 / 178.76	4.285	0.565	19.083	0.575	7.467	0.585	21.323	0.590	11.281
271	A	18.41 / 338.93	9.700	0.540	-6.837	0.555	57.168	0.645	161.949	0.720	9.171
	B	18.41 / 338.93	8.200	0.540	-1.337	0.555	39.168	0.645	173.949	0.720	11.171
	C	18.41 / 338.93	7.100	0.540	34.763	0.555	18.168	0.645	161.949	0.720	9.171
272	A	23.03 / 530.4	11.300	0.540	53.163	0.570	40.340	0.805	381.949	1.2	38.801
	B	23.03 / 530.4	9.800	0.540	51.663	0.570	21.340	0.805	390.959	1.2	51.801
	C	23.03 / 530.4	15.700	0.540	57.763	0.570	29.340	0.805	376.959	1.2	45.801

TABLE VII (Continued)

Run Number	Tap	W lb/h $\times 10^{-3} / \left(\frac{W}{10^3}\right)^2$	Static Δp_{5-7}	$\bar{v}$	Fuel Downpass Friction Δp_{7-8}	$\bar{v}$	Fuel Bottom Turn Friction Δp_{8-10}	$\bar{v}$	Fuel Uppass Friction Δp_{10-11}	$\bar{v}$	Exit Fuel → Start Riser Friction Δp_{11-14}
245	A	2.04/ 4.16	0.099	0.545	0.388	0.535	0.427	0.540	1.681	0.550	0.145
	B	2.04/ 4.16	0.032	0.545	0.505	0.535	0.241	0.540	1.908	0.550	0.054
	C	2.04/ 4.16	0.016	0.545	0.583	0.535	0.186	0.540	1.958	0.550	0.005
246	A	3.11/ 9.67	0.392	0.550	1.091	0.535	0.473	0.545	4.283	0.555	0.254
	B	3.11/ 9.67	0.344	0.550	1.148	0.535	0.328	0.545	4.451	0.555	0.222
	C	3.11/ 9.67	0.354	0.550	1.174	0.535	0.283	0.545	4.460	0.555	0.222
237	A	3.34/11.16	0.776	0.535	0.005	0.535	0.211	0.535	3.923	0.535	0.724
	B	3.34/11.16	0.333	0.535	0.392	0.535	0.048	0.535	4.064	0.535	0.792
	C	3.34/11.16	0.392	0.535	0.429	0.535	0.179	0.535	3.892	0.535	0.737
213A	A	3.98/15.84	0.861	0.500	0.003	0.475	0.446	0.485	4.677	0.495	1.133
	B	3.98/15.84	0.501	0.500	0.348	0.475	0.183	0.485	4.949	0.495	1.133
	C	3.98/15.84	0.596	0.500	0.398	0.475	0.265	0.485	4.722	0.495	1.133
236	A	4.21/17.72	0.690	0.560	1.606	0.560	0.460	0.570	6.815	0.570	0.642
	B	4.21/17.72	0.582	0.560	1.651	0.560	0.205	0.570	7.246	0.570	0.529
	C	4.21/17.72	0.759	0.560	1.537	0.560	0.301	0.570	7.087	0.570	0.529
234	A	5.20/27.04	0.664	0.550	2.646	0.550	1.134	0.555	10.286	0.555	
	B	5.20/27.04	0.584	0.550	2.672	0.550	0.802	0.555	10.672	0.555	
	C	5.20/27.04	0.888	0.550	2.695	0.550	0.816	0.555	9.831	0.555	
239	A	5.21/27.14	0.882	0.550	2.259	0.550	1.072	0.555	11.134	0.560	0.914
	B	5.21/27.14	0.550	0.550	2.296	0.550	0.417	0.555	10.749	0.560	2.113
	C	5.21/27.14	0.882	0.550	2.259	0.550	0.666	0.555	10.740	0.560	1.578
221	A	5.49/30.14									
	B	5.49/30.14									
	C	5.49/30.14									
101	A	5.62/31.58	1.226	0.465	2.798	0.465	1.610	0.470	13.508	0.470	
	B	5.62/31.58	1.266	0.465	2.254	0.465	1.110	0.470	14.012	0.470	
	C	5.62/31.58	1.148	0.465	2.876	0.465	1.610	0.470	13.008	0.470	

TABLE VIII

TOTAL FRICTIONAL PRESSURE LOSS NORMALIZED TO 650°F, 1000 psia. (Equation 34)

P_{20} psia	Run Number	W $\frac{lb}{h}$ × 10-3	Average Pressures, Temperatures, Specific Volumes						$\Sigma r\upsilon$ (3)	Δp_T Total psi Measured Taps 1-9	Essentially υ Constant Runs		Eq (34) $\Delta p_{T=C}$ (2) psi Calculated at Constant $\upsilon_{1000\ psi\ 650°F}$	Water Level in Vessel
			Taps 1-5 Downcomer		Taps 5-14 Fuel		Taps 14-19 Riser and Exit				$\bar{\upsilon}$ of Entire Bundle	$\Delta p_{T=C}$ (1)		
			P/T	$\bar{\upsilon}_D$	P/T	$\bar{\upsilon}_F$	P/T	$\bar{\upsilon}_R$						
1014	246	3.11	1014/660	0.570	1011/645	0.555	1006/648	0.560	0.557	8.64	0.562	8.67	8.75	None
1011	239	5.21	1009/645	0.555	998/635	0.550	991/635	0.555	0.551	21.62	0.552	22.1	22.1	None
1014	236	4.21	1014/664	0.570	1007/658	0.565	1001/653	0.565	0.566	13.70	0.567	13.7	13.7	None
1013	235	6.11	1011/668	0.575	998/665	0.580	984/661	0.585	0.580	29.73	0.580	29.0	29.0	None
1012	270	13.37	1005/643	0.555	944/606	0.565	882/596	0.600	0.568	139.6	0.573	137.5	139.0	17'-4"
995	213A	3.98	994/595	0.515	985/585	0.500	974/575	0.505	0.502	20.99	0.507	23.4	23.6	None
903	108	8.47	900/572	0.552	875/545	0.540	849/535	0.550	0.543	57.3	0.547	59.2	59.6	< 13'
980	103	10.72	975/560	0.485	938/547	0.485	901/540	0.510	0.488	84.2	0.493	96.5	97.5	15'-16'
926	109	13.37	921/593	0.565	876/578	0.585	839/563	0.600	0.584	87.7			84.8	< 13'
1011	271	18.41	991/626	0.545	851/587	0.615	703/569	0.750	0.623	318.8			289.5	17'
1015	272	23.03	971/608	0.545	665/541	0.765	361/501	1.44	0.820	697.8			482.0	18'-6"
1006	269	13.37	997/622	0.535	934/599	0.560	870/585	0.595	0.561	144.8			145.8	18'
1021	245	2.04	1021/663	0.565	1019/638	0.545	1017/648	0.550	0.548	3.91			4.03	None
1017	237	3.34	1017/630	0.535	1013/627	0.535	1009/623	0.530		7.98	0.533	8.46		None
1000	101	5.62	998/565	0.470	987/555	0.470	975/550	0.470		25.80	0.470	31.0		15'-18'
1015	234	5.20	1014/640	0.545	1003/640	0.555	992/640	0.555	0.554	24.80	0.552	25.30	25.3	None
1012	220	9.88	1006/600	0.510	974/595	0.525	941/593	0.545	0.526	76.87			82.6	None
1012	221	5.49	1011/593	0.500	1003/590	0.500	996/590	0.500		17.68	0.500	20.0		None

(1) $\Delta p_{T=C} = \frac{\bar{\upsilon}_C}{\bar{\upsilon}} \Delta p_{T_V}$

(2) $\Delta p_{T=C=650°} = \frac{\bar{\upsilon}_C \frac{1000\ psia}{650°F}}{\Sigma r\upsilon} \times (\Delta p_T) = \frac{0.565}{\Sigma(r\upsilon)} \Delta p_T$

(3) $\Sigma r\upsilon$ by Equation 34

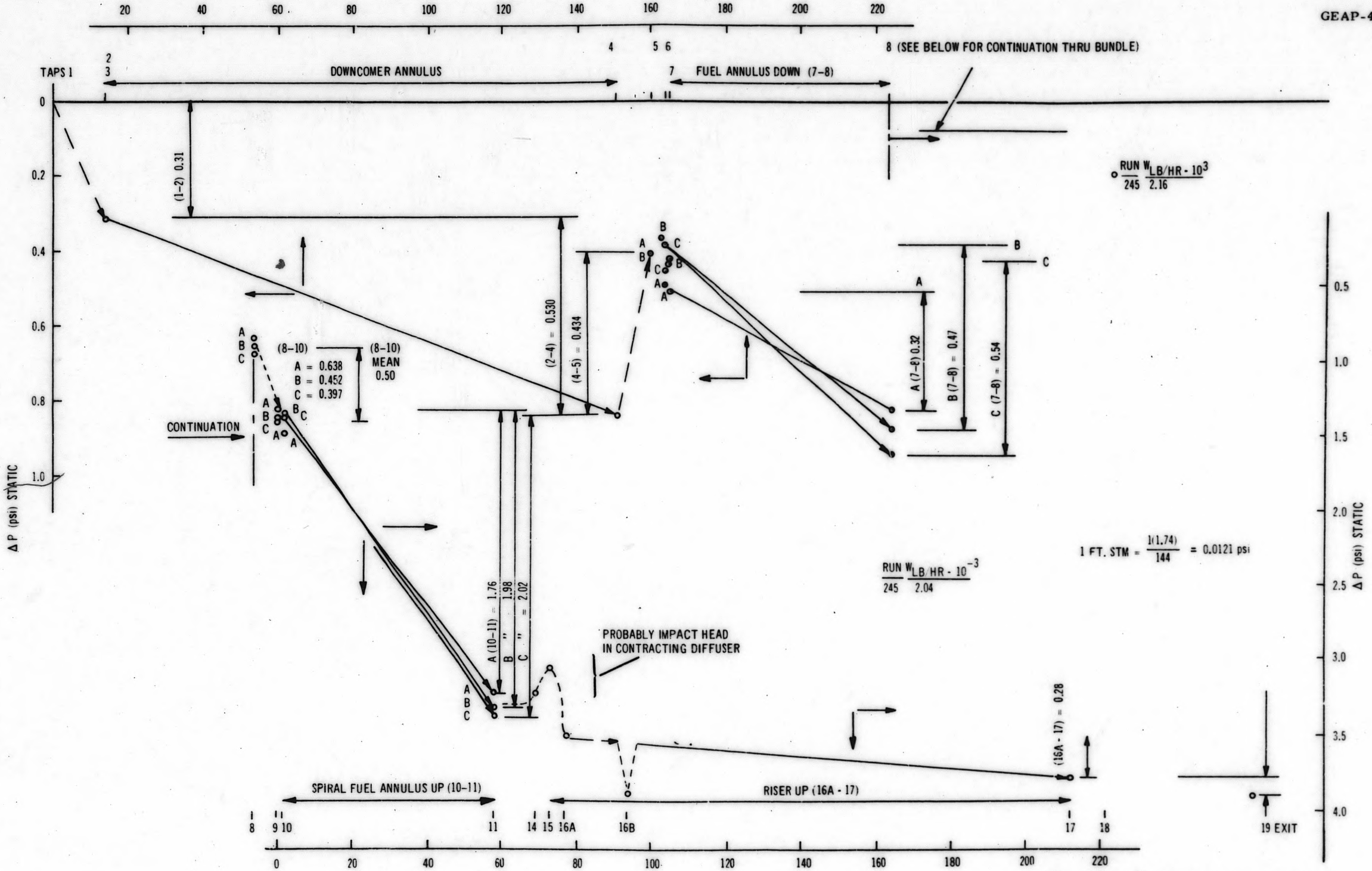

Figure 23. Typical Static Pressure Profile

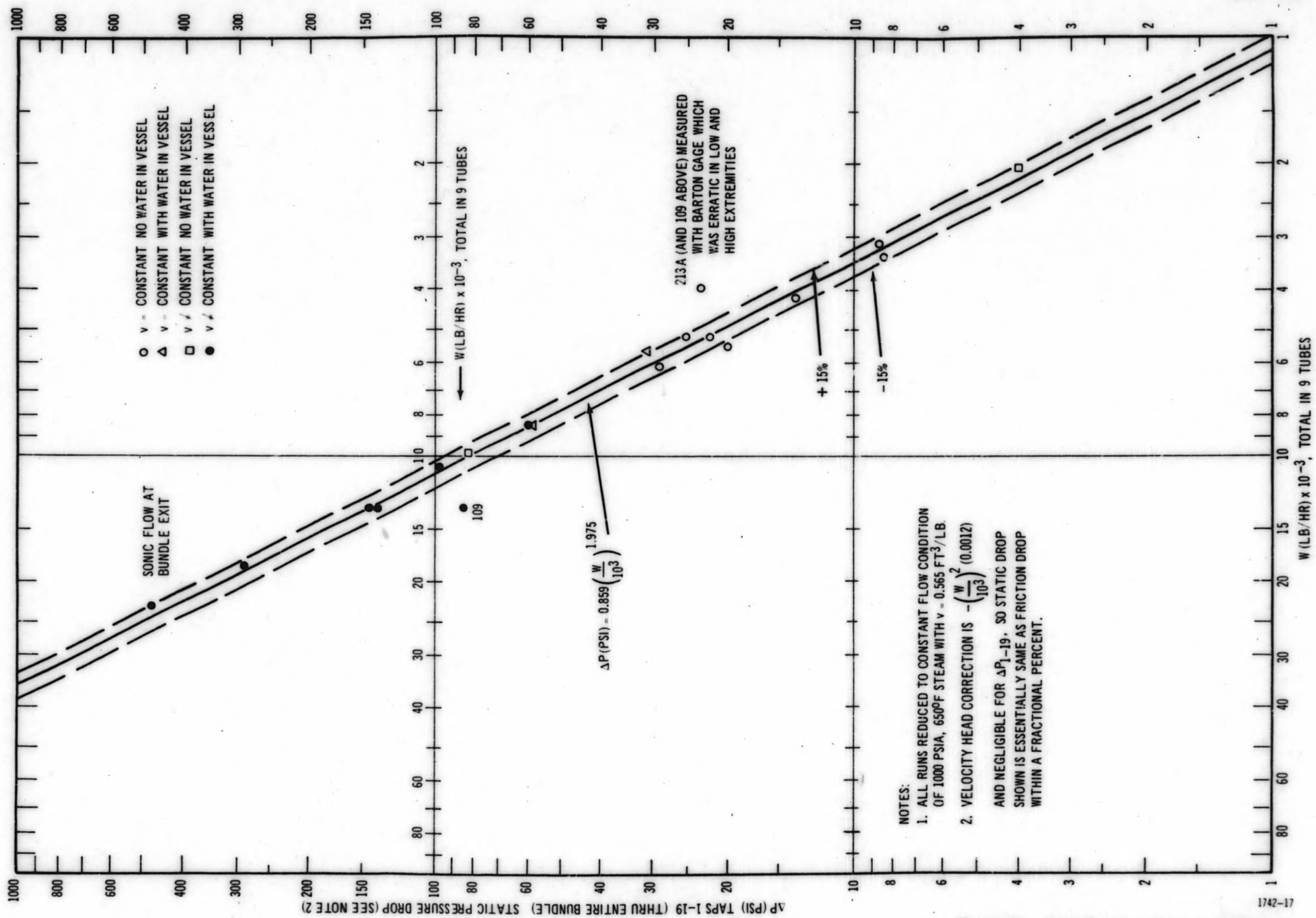

Figure 24. Total Pressure Drop in VESR Fuel Bundle MKI

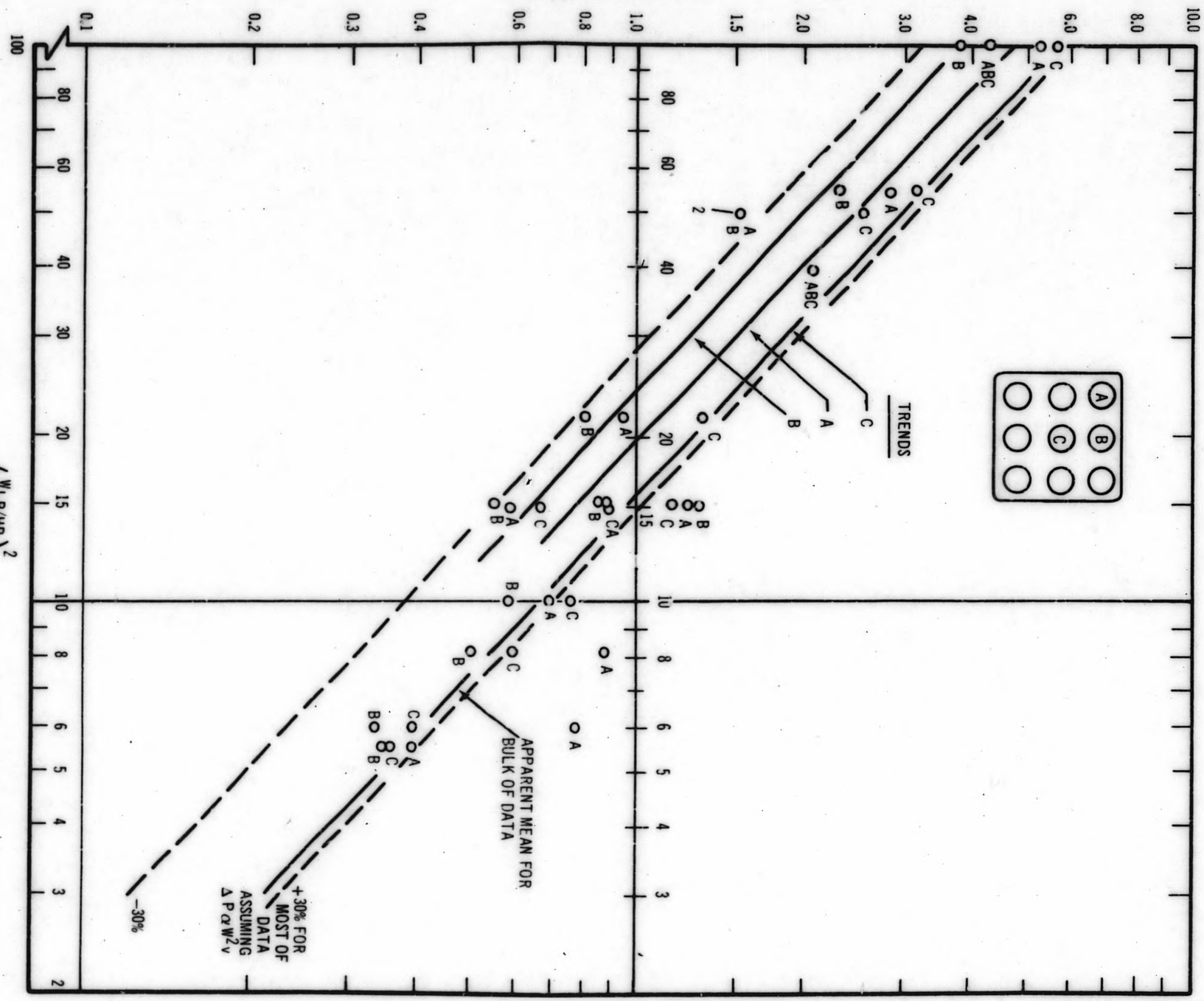

Figure 25. Static Pressure Drop - Plenum to Start of Fuel Downpass

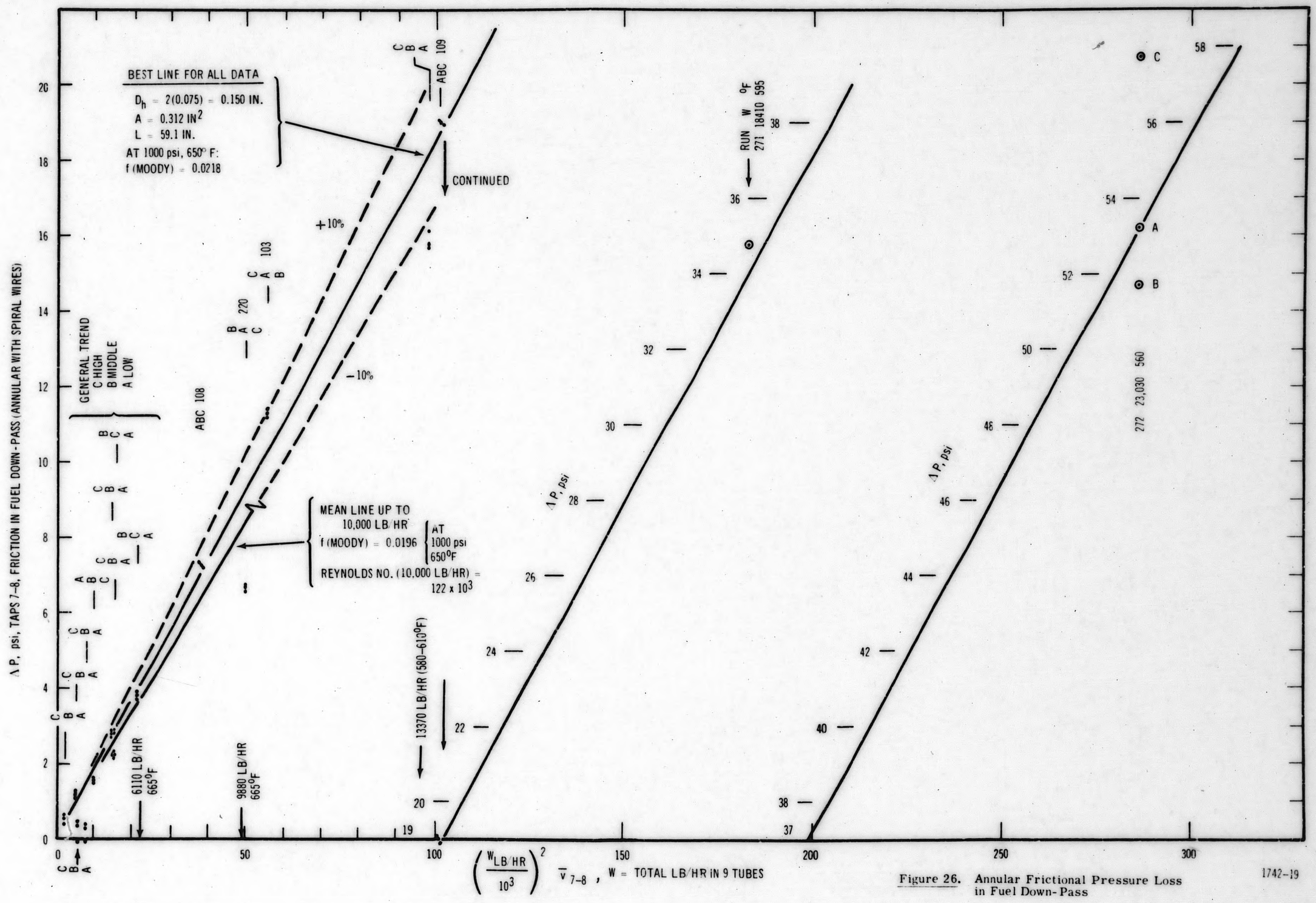

Figure 26. Annular Frictional Pressure Loss in Fuel Down-Pass

1742-19

1742-20

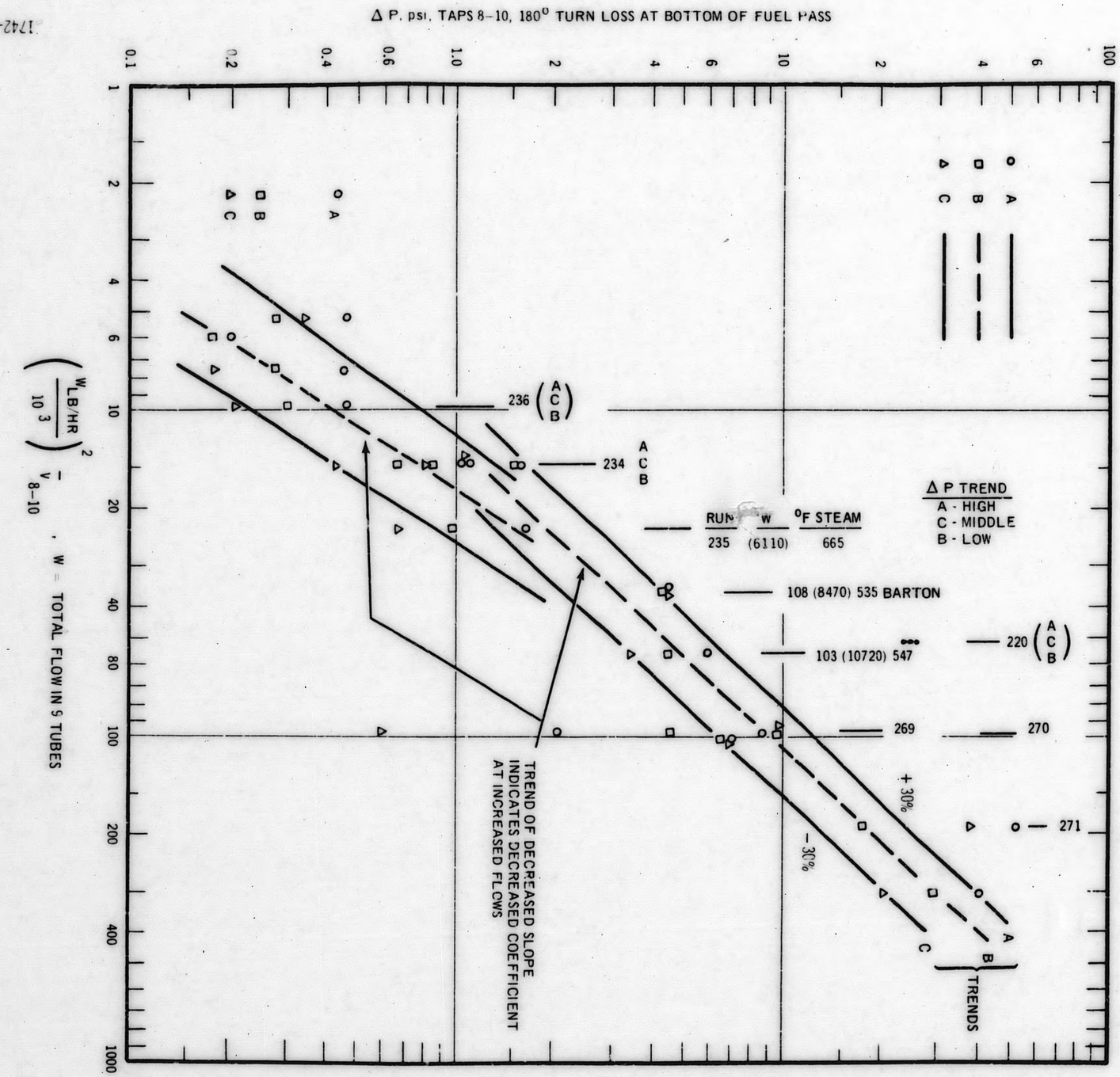

Figure 27. Frictional Pressure Loss at 180° Turn and Contraction at Bottom Fuel

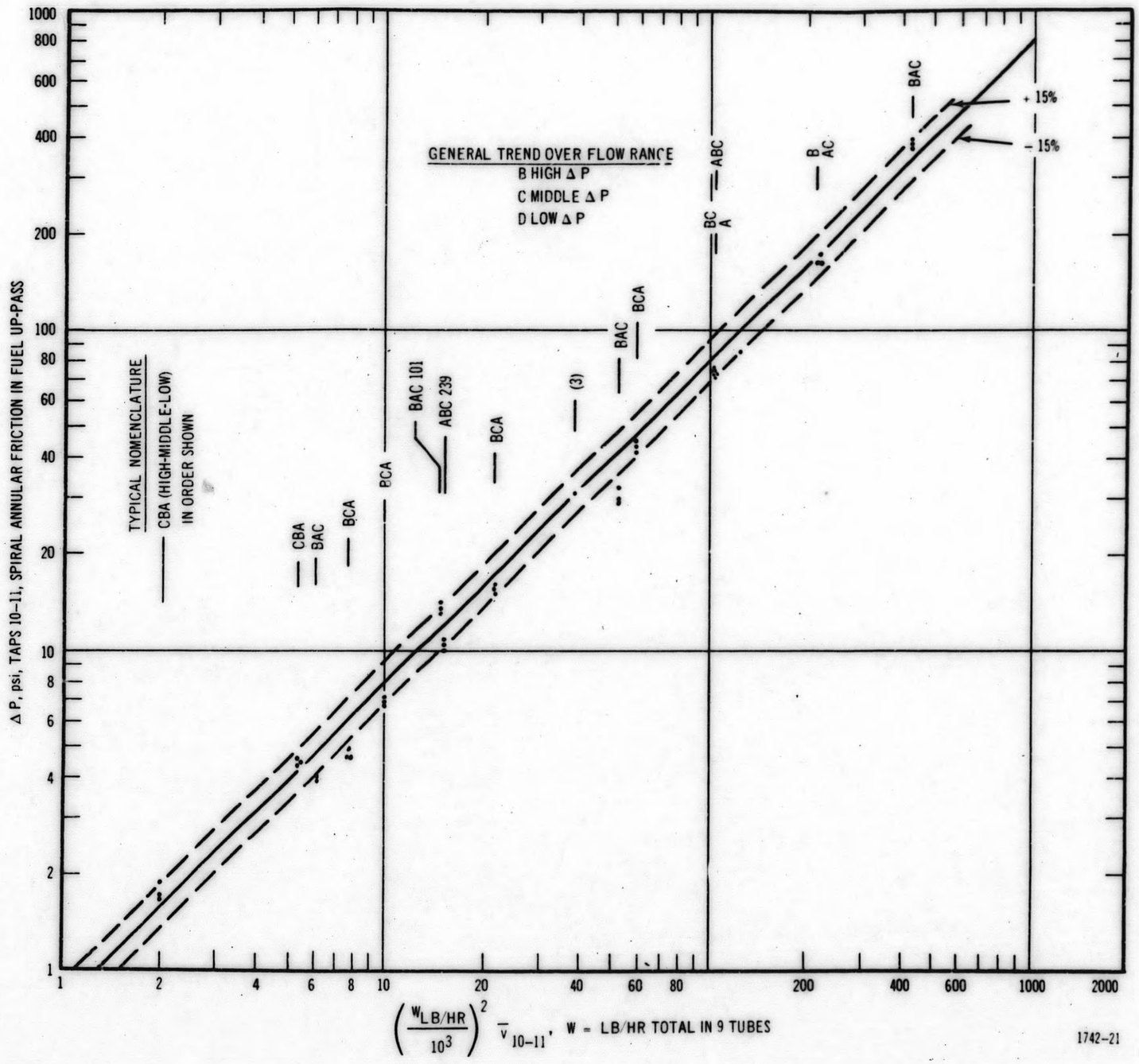

Figure 28. Spiral Annular Friction Pressure Loss in Fuel Up-Pass (Total Flow Range Tested)

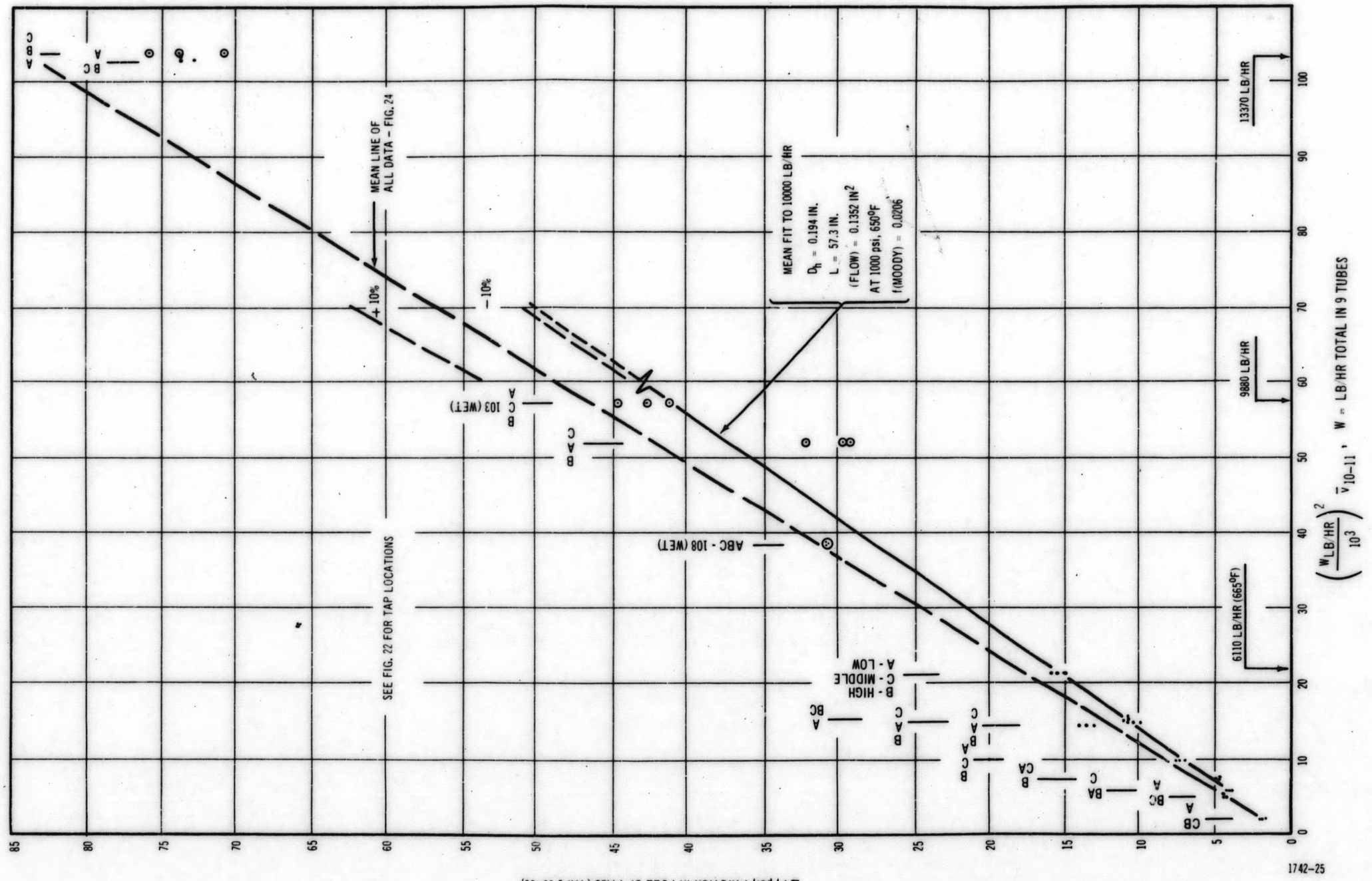

Figure 29. Friction Pressure Loss in Fuel Up-Pass (0-13,000 lb/h Range)

6-63/6-64

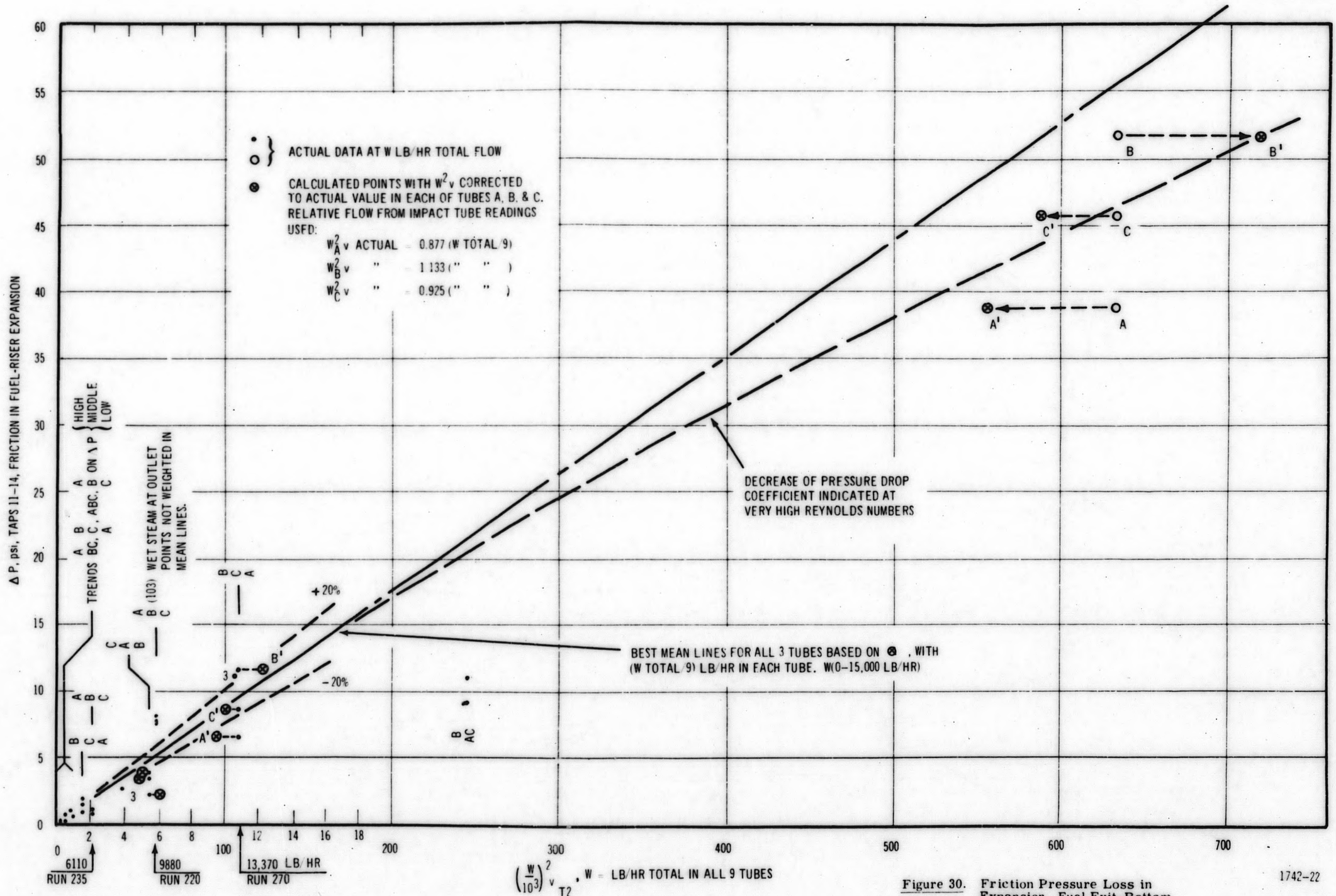

Figure 30. Friction Pressure Loss in Expansion, Fuel Exit-Bottom Riser (0-13,000 lb/h)

1742-22

6-65/6-66

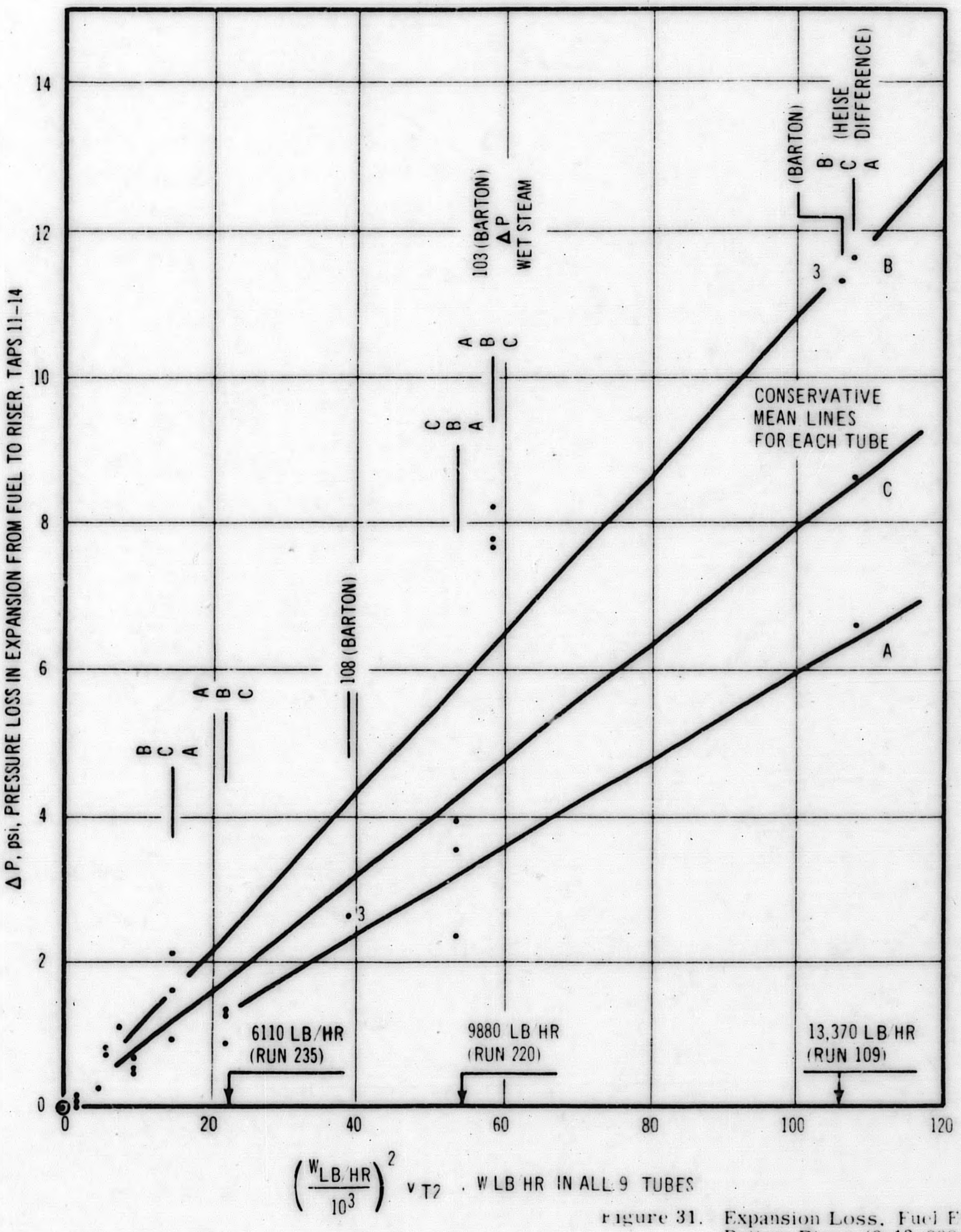

Figure 31. Expansion Loss, Fuel Exit - Bottom Riser (0-13,000 lb/hr)

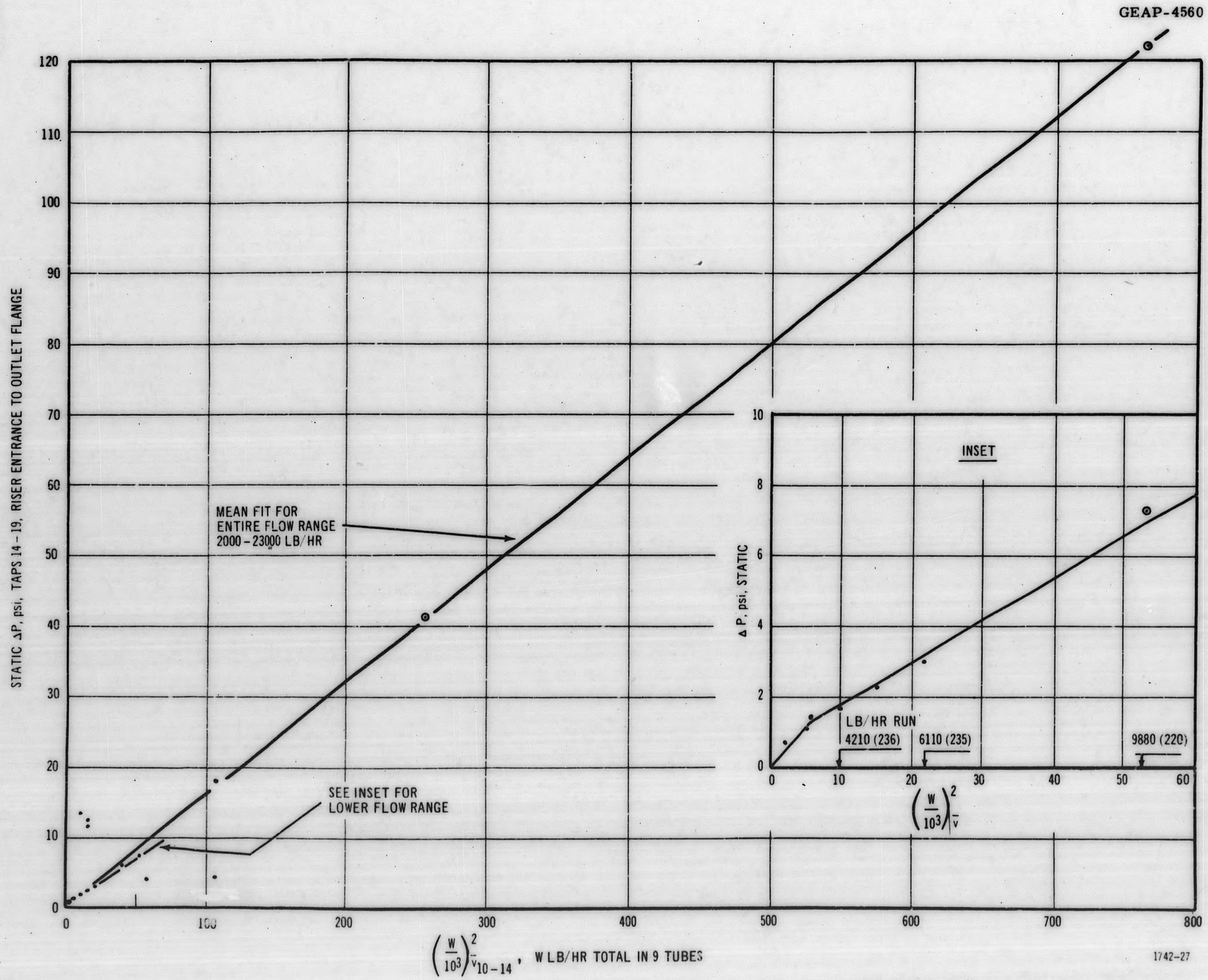

Figure 32. Static Pressure Drop, Riser-Exit Flange

The balance of figures, are on the whole, self-explanatory. Most of the various losses correlated well as a straight line with $w^2\overline{v}$, indicating the coefficient was essentially constant over the Reynolds numbers tested. Three of the component pressure losses indicated a decrease of pressure loss coefficient with flow. These were the loss in the turn at the bottom of the fuel pass (Figure 27); the fuel-riser expansion (Figure 30); and the riser and exit pipe loss (Figure 32).

It may be noted that the general trend of relative pressure loss between tubes A, B, and C in the two fuel pass (Figures 26 and 28) shows a strong trend of high-low in the sequence B, C, A. This agrees with the high-low sequence, obtained with the Pitot tubes, in Section VI.

The losses for each of the unique tubes, in Figure 30 for example, are plotted versus the total flow in all nine tubes. Thus, more scatter is obtained in the data as plotted, than is inherent, due to mass flow distribution among the tubes. That is, it will correlate somewhat better if allowance is made for flow variation. This was done for a few points as shown on Figure 30, and the correction draws most of the points within ±20 percent of the mean straight line drawn.

SECTION VII

DISCUSSION OF RESULTS

For a discussion of results, refer to the specific headings under Section VI, Results and Discussions.

REFERENCES

1. Fluid Meters - Their Theory and Application, Report of ASME Research Committee, 5th ed., 1959.

2. Merriam Standard Indicating Fluids Brochure IM-11.

3. Keenan and Keyes, "Thermodynamic Properties of Steam," J. Wiley, 31st Printing, 1958.

4. Vargaftik, Smirnova, and Timroth, Steam Properties Presented in ANL6213, by J. Heineman.

END